



Research paper

A review of Pakistani shales for shale gas exploration and comparison to North American shale plays

Ghulam Mohyuddin Sohail^a, Ahmed E. Radwan^{b,*}, Mohamed Mahmoud^{c,*}

^a Department of Geological Engineering, University of Engineering & Technology, Lahore, Pakistan

^b Faculty of Geography and Geology, Institute of Geological Sciences, Jagiellonian University, ronostajowa 3a, 30-387 Krakow, Poland

^c Petroleum Engineering Department, CPG, KFUPM, Saudi Arabia



ARTICLE INFO

Article history:

Received 18 November 2021

Received in revised form 21 April 2022

Accepted 27 April 2022

Available online xxxx

Keywords:

North America shale gas

Pakistan shale gas

Indus Basin

Shale gas

Unconventional resources

ABSTRACT

Recent advancements in technologies to produce natural gas from shales at economic rates has revealed new horizons for hydrocarbon exploration and development worldwide. The importance of shale oil and gas has aroused worldwide interest after the great success of production in North America. In this study, different marine source rocks of Pakistan are evaluated for their shale gas potential using analogs selected from various North American shales for which data have been published. Pakistani formations reviewed are the Datta (shaly sandstone), Hangu (sandy shale), Patala (sandy shale), Ranikot (shaly sandstone), Sembar (sandy shale) and Lower Goru (shaly sandstone) formations, all of which are known source rocks in the Indus Basin. Available geological data of twenty-six wells (e.g., geological age, depositional environment, lithology and thickness), geochemical data (e.g., total organic carbon (TOC), vitrinite reflectance (Ro), rock pyrolysis analysis and maturity), petrophysical data (e.g., porosity and permeability) and dynamic elastic parameters estimated from logs (Young's modulus and Poisson's ratio) have been investigated. According to this study, the Pakistani shales are explicitly correlated with the most active shale gas plays of North America. The burial depths or geological position of the Pakistani shales are generally comparable to or slightly higher than the North American shales based on the available data. The thicknesses of the Pakistani (except for the Sembar shale) and North American shales fall in similar ranges. In terms of mineralogical composition, all of the Pakistani shales except the Ranikot and Hangu shales have quartz contents in the 40% to 50% range (approximately), which is similar to most of the North American shales. The high maximum TOC of the Hangu and Sembar shales (10%) is comparable to the New Albany, Antrim and Duvernay shales. The maximum TOC values for the Ranikot (3%), Lower Goru (1.5%) and Datta (2%) shales are lower than all North American shales. The TOC of Patal Shale (~5%–10%) is comparable to Fayetteville and Eagle Ford shales. The geological and geochemical parameters of all the Pakistani shales reviewed in this work are promising regarding their shale gas prospects. However, geomechanical data are required before conclusions on these shales' economic production can be made with confidence.

© 2022 The Author(s). Published by Elsevier Ltd. This is an open access article under the CC BY-NC-ND license (<http://creativecommons.org/licenses/by-nc-nd/4.0/>).

1. Introduction

The recent advancement of the unconventional petroleum systems especially that target source-rock reservoir i.e. organic-rich mudstone that act source as well as reservoir rock at the same time, has led to a re-evaluation of basic and important geological processes that are functioning in finegrained sedimentary rocks (Jarvie, 2012; Taylor and Macquaker, 2014). Understanding the geological, geochemical, and geomechanical characteristics of shale rocks is fundamental to safe drilling (e.g., Radwan et al.,

2019, 2020, 2021, 2022; Cui and Radwan, 2022; Radwan, 2021; Xie et al., 2022; Abdelghany et al., 2021), performing exploration tasks (e.g., Vengosh et al., 2013; Hao et al., 2013; Naizhen and Guoyong, 2016; Liu et al., 2019; Wenzhi et al., 2020), and reaching optimized production (e.g., Maxwell, 2011; Martinez-Gomez et al., 2017). After the first commercial natural gas discovery from Devonian organic-rich shale in the US in 1821, shale hydrocarbon resources have gained more attention in North America as a key energy resource (Curtis, 2002; Jarvie et al., 2007; Chalmers and Bustin, 2008). In Asia, particularly large shale gas plays were discovered in China where the Cambrian, Ordovician-Silurian, Carboniferous-Permian and Triassic-Jurassic shales are the most significant producing resources (Zou et al., 2010; Hao et al., 2013; Caineng et al., 2015). Other shale plays exist across the Asian

* Corresponding authors.

E-mail addresses: gmdsohail@uet.edu.pk (G.M. Sohail),

radwanae@yahoo.com (A.E. Radwan), mmahmoud@kfupm.edu.sa (M. Mahmoud).

continent and more development plans are going forward to discover more resources in many countries such as India and Saudi Arabia (e.g., [Mustafa et al., 2022](#)). The energy crisis in Pakistan needs a long-term solution to reduce the gap between supply and demand because production from conventional reservoirs is insufficient to fulfill the country's growing demand for energy ([Abbasi et al., 2014](#)). According to initial studies of the United States Energy Information Administration, Pakistan contains approximately 3000 bcm (billion cubic meters) of shale gas reserves ([US EIA, 2015](#)). [Abbasi et al. \(2014\)](#) suggest that shale gas's total resource potential in Pakistan is higher than the estimated reserve.

The exploitation of shale gas reservoirs may enhance gas production and reduce the severity of the ongoing energy crisis. The main challenge in Pakistan is to evaluate the shales using limited data and samples. That is why only a few companies are working on shale gas reservoirs in Pakistan now. The researchers need to assess and rank prospective Pakistani shales to entice companies to consider shale gas development. The geological characterization of Pakistani shales has been investigated by several authors (e.g., [Warwick et al., 1995](#); [Kazmi and Abbasi, 2008](#); [Ahmad et al., 2012](#); [Hakro and Baig, 2013](#); [Jalees, 2014](#)), but detailed work is required on geochemical, petrophysical and geomechanical characterization for assessing the actual potential of shales in Pakistan ([Abbasi et al., 2014](#)).

Shale gas development in the U.S.A. and Canada has been active for nearly two decades, and the characterization of several important shales has reached a mature state (see [Fig. 1c](#) for the location of North American shale plays). Though there are no single, well-defined standard values for various properties that enable quantification of shale gas potential ([Wang and Wang, 2016](#)), comparing unproven prospects against various properties measured on known shale gas producers serves as a useful basis for screening shale gas candidates. Thus, an integrated comparison has been undertaken in this work to assess the shale gas potential of various Pakistani shales and identify critical data gaps that must be addressed to achieve a more positive assessment in the future.

This comparison included the thickness, burial depth, mineralogy, total organic carbon (TOC), vitrinite reflectance (Ro), and porosity, all of which have been published for both North American shale gas reservoirs and Pakistani shale gas candidates. Further, the data compilation included permeability and selected mechanical properties (Poisson's ratio and Young's modulus) for the North American shales. However, data for these properties were found to be unavailable for the Pakistani shales. Thus, the work presented here expands upon previous comparative studies of Pakistani and North American shales undertaken by [Ayaz et al. \(2012\)](#) and [Haider et al. \(2012\)](#), in that additional shales with the actual thickness of shales in shale formation are considered, and more emphasis is placed on identifying data gaps (e.g., regarding mechanical properties and preservation conditions) which should be addressed in future research (see [Fig. -1d](#) for additional shales).

1.1. Geology of study area

Three sedimentary basins exist within Pakistan namely: The Indus Basin, the Balochistan Basin, and the Pishin Basin. Most conventional oil and gas production occurs in the Indus Basin ([Kazmi and Abbasi, 2008](#)), which is subdivided into three parts, i.e., the Upper, Middle and Lower Indus Basins (UIB, MIB and LIB, respectively) – see [Fig. 1a](#) and [b](#). Though the Lower Indus Basin (LIB) is likely more prospective for hydrocarbon production, most of the marine shales of Indus Basin, as encircled in [Fig. 1d](#), have been demonstrated to be source rocks for conventional reservoirs in the basin ([Kadri, 1995](#)). As such, it seems reasonable to assess their potential for shale gas production.

Table 1

Selected shale gas formations of Pakistan ([Sohail, 2020](#)).

Shale gas formation	TRR (bcm)
Datta	N.A.
Hangu	N.A.
Patala	N.A.
Sembar	2860 (US EIA, 2015)
Ranikot	125 (US EIA, 2015)
Lower Goru	N.A.

TRR: Technically recoverable reserves, bcm: billion cubic meter

N.A.: Not available.

2. Materials and methods

Relevant data for Pakistani and North American shales were collected from published literature, and the Pakistani shales data were further assessed and supplemented using well logs and geochemical (Rock-Eval Pyrolysis, Vitrinite reflectance) data. The available and interpreted data of six Pakistani shales are summarized in [Tables 1, 2](#) and [3](#). The depth and thickness of different Pakistani shales formations were established from available well data and generalized stratigraphy of the relevant part of the Indus Basin. Then, shale intervals were identified using gamma-ray (GR) log and added up to get the total thickness of shale in each shale formation (see [Fig. 1](#) for well locations, and [Figs. 2](#) and [3](#) for depth and thickness of Pakistani shales, respectively). In [Fig. 3a](#), the above procedure of shale identification from the GR log is explained and the total shale thickness in a particular well is given in [Table 2](#).

Burial History plots for U1 (drilled at Upper Indus Basin) and L6 (at Lower Indus Basin) wells were developed using the thicknesses, geological ages, and lithologies of each formation. The petroleum system information, kerogen type, and hydrogen index data were also incorporated to assess thermal maturity (e.g., estimated vitrinite reflectance) of Datta and Sembar Shales in wells U1 and L6, respectively. The essential data (e.g., periods of erosion and non-deposition, geothermal gradient, paleo-water depth, heat flow rate, basin latitude) were taken from the published literature of Indus Basin ([Kadri, 1995](#); [Wandrey et al., 2004](#); [Kazmi and Abbasi, 2008](#); [Siddiqui et al., 2014](#); [Saddique et al., 2016](#)).

The ternary plots of mineralogy were developed using local (single well) and regional scale (multiple wells) data and classifying the shales based on their siliceous, argillaceous and calcareous contents. Bar charts of depth, thickness, TOC, Ro, and porosity for six Pakistani and eight USA shales were developed for comparison.

The type, quality and maturity of kerogen in Pakistani shales were discussed through different standard plots (Hydrogen index versus Oxygen index (Van Krevlen diagram), TOC versus S₂). In addition, the characteristics of Pakistani shales were studied and discussed concerning other North American shales. The dataset of North American and Pakistani shales is summarized in [Appendix](#).

3. Geological and geochemical characteristics of Pakistani shales

Organic-matter-rich shales, the main target rocks for unconventional oil and gas exploration and development across the world, according to their origin, could be categorized into three types: marine, marine-continental transitional and continental shales ([Zou et al., 2010](#)). Six shale units are the major fine-grained sediments in Pakistan's sedimentary sequence, and their depositional environment varies. In Pakistan, organic-rich shales spanning in age from Pre-Cambrian to Quaternary were widely deposited. The geological characteristics are discussed per each shale rock units as the following:

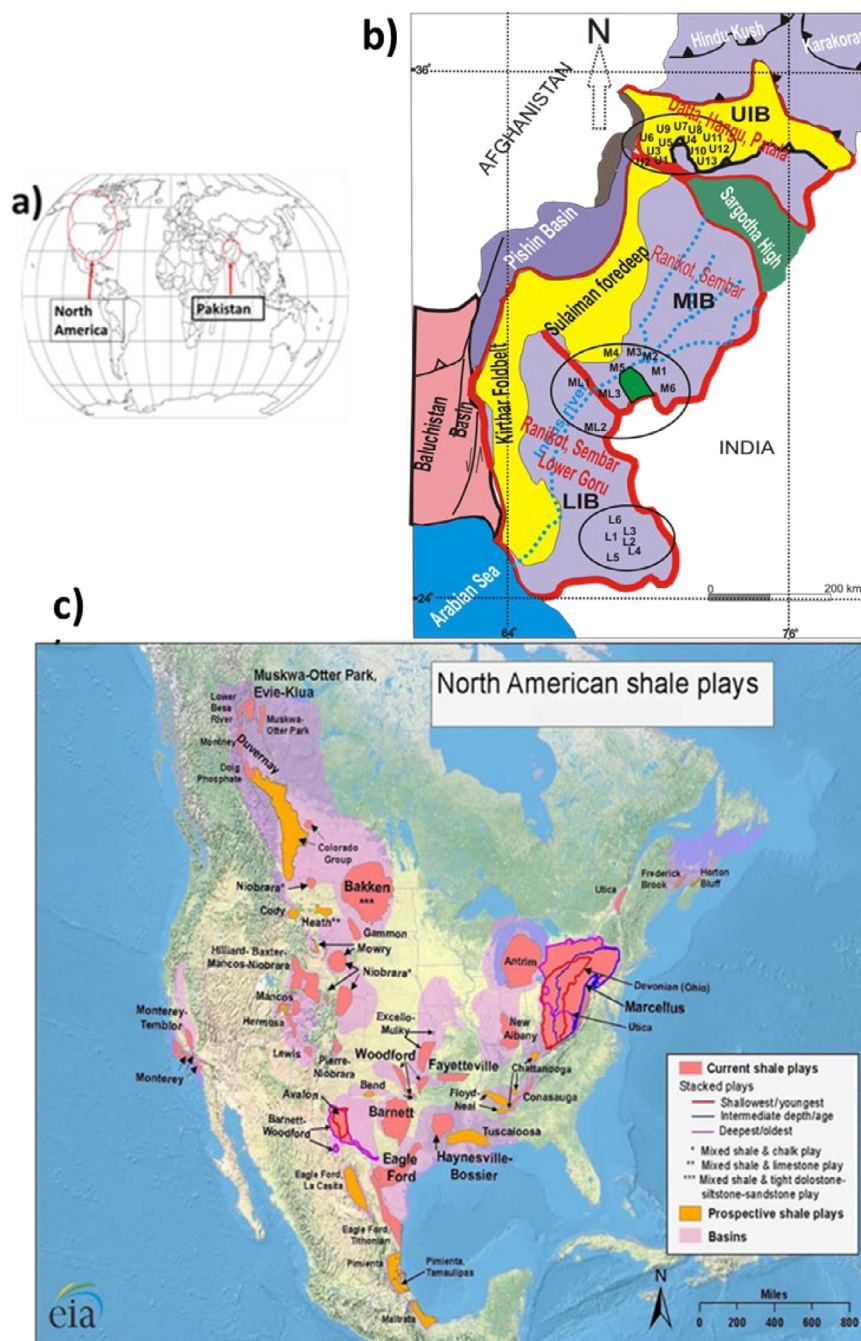


Fig. 1. (a) World map showing the general location of shale plays investigated in this work. (b) Map showing zones (encircled) for potential Pakistani shale plays in UIB (Upper Indus Basin), MIB (Middle Indus Basin) and LIB (Lower Indus Basin), U, ML and L represents different wells drilled in UIB (U), Middle-Lower (ML), and LIB (L), respectively (modified after <https://geology.com/world/pakistan-satellite-image.shtml> Sohail, 2020). (c) Map showing North American shale plays (modified after US EIA, 2011).

3.1. Hangu Formation

The Hangu Formation is belonging to the early Paleocene age and was deposited in a marginal marine environment. It is comprised of sandstone with minor mudstone, claystone, carbonaceous shale, and intercalations of limestone (Warwick et al., 1995). The depth and thickness of the shale intervals vary from 2700 m to 4500 m and 3 m to 32 m, respectively, as given in Table 2.

TOC (2%–10%) and Ro (0.81–1.3%) values are relatively high in this shale, and has high quartz (60%–70%) and low clay (<20%)

contents (Haider et al., 2012; Shah et al., 2013). The petrographic analysis of outcrop samples in the potential shale play zone of UIB (see Fig. 1b for location of potential zone) as given in Table 3, shows that the Kerogen is of Type-II and III with poor genetic potential (Shahzad, 2007). Hangu Shale cutting samples from U3 well (as given in Table 2) are organic-rich (TOC = 2.3%), and S1 & S2 values (7.78 and 5.78 mg/g rock) suggest very good hydrocarbons potential regarding generated and residual hydrocarbons, respectively. The Hydrogen index indicates organic matter derived from Type-II and Type-III Kerogen, as shown in Fig. 4a (257 mg/g TOC), which is consistent with the findings of

Era	Period	Tectonic	Formation	Deposition	Symbols	Lithology
Cenozoic	Neogene	Drifting/Passive Margins, Collision	Siwalik Group	Shallow to Deep marine		Fluviatile clastics, Conglomerate, Siltstone
			Unconformity			
	Hangu+Patala		Marine fossiliferous Limestone, Sandstone and Shale			
	Namma+Sakesar					
Paleocene/Eocene	Ranikot					
Mesozoic	Cretaceous	Rifting and Break-up of Gondwanaland	Unconformity	Shallow seas		Sandstone
			Goru			Shale
			Sember			Limestone
			Unconformity			
	Jurassic		Samana Suki/Chilton	Deep to Shallow marine		Sandstone
			Shinawari			Paralic Sandstone and Shale
			Datta			
	Triassic		Unconformity	Shallow marine		Dolomite
			Kingriali			Fluviatile Sandstone
			Tredian			Limestone, Sandstone and Shale
Mianwali						

Fig. -1d. Generalized Stratigraphy of Pakistan and encircled are the formations which contain thick shale layers which have been approved as source rocks in relevant basin (modified after Kadri, 1995; Sohail, 2020).

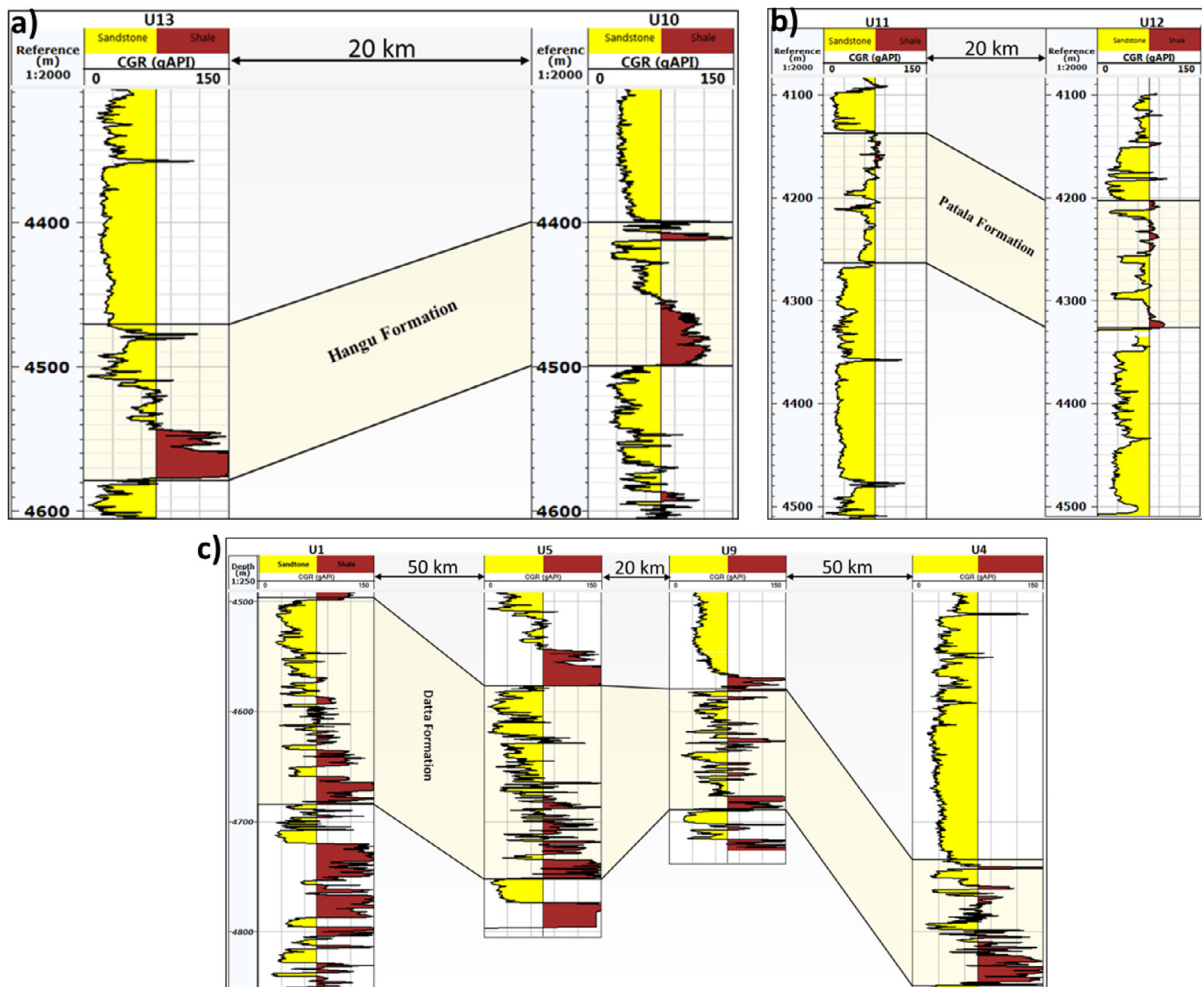


Fig. 2. Wells Correlation based on computed gamma ray log (CGR) for (a) Hangu, (b) Patala and (c) Datta Formations (see Fig. 1 for wells location) (modified after Sohail, 2020).

Table 2

Thickness of shale intervals in studied formations interpreted using GR log of studied wells (extracted from Sohail, 2020).

Basin	Formation	Well	Latitude (degrees)	Longitude (degrees)	Formation top (m)	Formation bottom (m)	Formation thickness (m)	Shale thickness based on this study (m)	Shale thickness in literature (m)	Technically recoverable reserve Trillion cubic feet (tcf)	
UIB	Datta	U1	33.23	71.51	4751	4795	44	6	6 to 70		
		U4	33.20	72.08	4730	4894	164	44			
		U5	33.14	71.98	4572	4726	154	54			
	Hangu	U8	32.96	73.01	2747	2752	5	5	Not available		
		U9	33.22	71.49	4424	4449	25	3			
		U10	32.97	72.66	2712	2729	17	10			
		U1	33.23	71.51	4475	4570	95	32			
		U3	32.87	71.94	2700	2750	50	5			
	Patala	U9	33.22	71.49	4203	4350	147	7	Not available		
		U11	32.94	72.66	2603	2625	22	10			
		U12	32.95	72.66	2620	2647	22	27			
		U13	33.12	72.99	3052	3120	68	26			
	Sembar	M1	29.11	71.39	2324	2346	22	17	Not available		105 (US EIA, 2015)
		M2	28.60	71.74	1040	1201	161	157			
		M3	30.40	70.46	1410	2167	757	550			
M4		30.25	67.58	796	833	37	37				
M5		28.14	69.96	3480	3530	50	50				
M6		28.03	70.85	1641	1664	23	23				
L6		27.46	69.34	3411	3550	139	80				
MIB/LIB	Ranikot	M1	29.11	71.39	1683	1765	81	64	Not available	4.4 (US EIA, 2015)	
		ML1	25.27	68.17	270	1095	825	214			
		ML2	26.28	67.46	1250	2000	750	165			
		ML3	28.15	70.23	1520	1680	160	33			
		M2	31.19	71.52	1916	2135	219	85			
Lower Goru	L1	26.98	69.20	2615	3639	1024	639	200 to 400			
	L2	27.00	68.76	2500	3550	1050	795				
	L3	27.18	69.24	3084	3485	401	389				
	L4	27.02	68.93	2696	3440	744	640				
	L5	25.57	68.39	2598	2800	202	198				
	L6	27.46	69.34	2260	3410	1150	768				

Asif (2010). The S2-TOC plot (Fig. 4c) shows the Type-III Kerogen, and the HI-Tmax plot shows (Fig. 4b) the Kerogen is thermally immature in Hangu Shale. The Kerogen may be thermally mature away from wells used in this study, as reported by Haider et al. (2012) and Shah et al. (2013), because the UIB was extensively disturbed compared to other parts of the Indus Basin due to tectonic activities.

3.2. Patala Formation

This formation is of the late Paleocene age, and it was deposited in an intertidal lagoonal environment. Its lithology is highly variable throughout the Indus Basin; it contains a high volume of organic-rich shale along with limestone (Jalees, 2014). The depth and thickness of shale intervals in the Patala Formation vary from 2600 m to 4200 m and 7 m to 33 m, respectively (Haider et al., 2012). It contains quartz (30%–40%), clay (25%–30%) and calcite (0%–20%), though in some wells the quartz contents are much higher (70%–80%) than clay and calcite (Jalees, 2014). The values of S1 range between 0.5 to 3 mg HC/g rock, and values of S2 lie in the range between 6.5–19 mg HC/g rock, indicating fair to very good and good to very good quality, respectively, as given in Table 3. Van Krevlen diagram and S2-TOC (Fig. 4a and c) plots elucidate that the Patala shale contains Type-III Kerogen and has the potential to produce gas only. Published studies based on wells data show excellent TOC (~5%–10%) with thermally mature Kerogen of Type II/III (Jalees, 2014). Although the Tmax of the Patala Formation was in the early to main stage oil window maturity (Fig. 4b), the formation may act as a minor gas source in studied wells.

3.3. Datta Formation

The Lower Jurassic Datta Formation was deposited in a delta plain setting of a fluvial-dominated delta. Facies variations reflect that marine conditions prevailed in some parts of the UIB (Kazmi and Abbasi, 2008). It is comprised of sandstone interbedded with siltstone, shale, carbonaceous clays and coal stringers (Kazmi and Abbasi, 2008). The shale interval's depths are 4640 m to 4700 m, with thicknesses in the 6 m to 54 m range. These shale intervals contain high quartz (>50%) and low clay contents (10%–20%) (Gul et al., 2016). The shale of the Datta formation (in the whole Upper Indus Basin) has fair-to-good source rock potential based on its total organic carbon content (TOC = 0.5%–2%) and contains whole oil window maturity based on vitrinite reflectance (Ro = 0.5–0.55%) (Khalid et al., 2015). The TOC values range 1.73% to 3.73% in the studied wells indicating good to very good quality kerogen. The S1 (0.05–0.18) and S2 (0.30–0.56) values are poor (see Table 3). Van Krevlen diagram and S2-TOC plots elucidate that the Datta Shale contains Type-III Kerogen and has the potential to produce gas only. Kerogen is generally of Type-II, and a mixture of Type-II and Type-I is also present. The Tmax-HI plot shows the kerogen is thermally mature in studied wells, and the Datta Formation had entered the gas generation window at U1-well, as shown in Fig. 5.

3.4. Sembar Formation

The Lower Cretaceous Sembar Formation is exposed at the boundary of MIB and LIB and is composed of shale with minor siltstones and sandstones (Kazmi and Abbasi, 2008; Ahmad et al.,

Table 3
Geochemical data for Pakistani shales (Sources of data are given in the last column; Sohail, 2020).

Pakistani shale	Location	Rock-Eval Pyrolysis									Vitrinite Reflectance (Ro) and Maceral Analysis				
		TOC	S1	S2	S3	Tmax	GP = S1 + S2	PI = S1/(S1 + S2)	OI	HI	Ro	Petrographic analysis	Kerogen type and Maturity stage	Reference	
		%	mg HC/g rock	mg HC/g rock	mg HC/g rock	°C	mg HC/g rock	unitless	mg CO ₂ /g TOC	mg HC/g TOC	%				
Hangu	Outcrop	2.3	0.14	0.39	1.1	427	0.5	0.26	49	17	0.5	Vitrinite (≥50%), Inertinite (<20%)	Marginally mature	Shahzad (2007)	
		1.8	0.08	0.05	0.6	432	0.1	0.62	33	3	0.9	Vitrinite (≥50%), Inertinite (<20%)	III and IV		
		2	0.07	1.48	0	421	1.6	0.05	2	76	0.5	Vitrinite (≥50%), Inertinite (<20%) Liptinite (<5%)	Marginally mature		
	Well	Depth													
	U3	4692–94	2.3	7.78	5.78	–	–	13.56	0.57	–	257	–	–	II and III	Asif (2010)
Patala	Outcrop	2	0.04	0.08	0.4	433	0.12	0.33	22	4	–	–	–	Shahzad (2007)	
		1.8	0.09	0.04	0.3	380	0.13	0.69	17	2	–	–	–		
		2.3	0.15	0.13	1.4	380	0.3	0.54	62	6	0.5	Vitrinite (≥50%), Inertinite (<20%)	II and III, marginally mature		
	Well	Depth													
	U12	2630	10	3	19	0.7	444	21	0.42	49	100	–	–	III, gas prone	Jalees (2014)
	U13	3062	5	0.5	6.5	0.7	440	11.5	0.3	220	200	–	–	III, minor oil and gas potential	
Datta	Outcrop	0.8	0.05	0.13	0.3	430	0.2	0.28	35	16	0.5	Vitrinite (≥50%) Inertinite (<5%)	Marginally mature	Shahzad (2007)	
		1.1	0.24	0.31	0.3	430	0.5	0.53	30	20	–	Inertinite (≥50%) Liptinite (<5%) Vitrinite absent	II, oil window		
		1	0.04	0.1	0.3	432	0.1	0.29	32	10	0.7	Vitrinite (≥50%) Inertinite (<20%) Liptinite (<20%)	III, peak maturation		
			TOC	S1	S2	S3	Tmax	GP	PI	OI	HI	Ro	Petrographic analysis	Kerogen Type and Maturity Stage	Ref.
	Well	Depth													
	U1	4605–07	1	0.05	0.36	1.06	456	0.41	0.12	106	36	0.5	–	II/III	Jalees (2014), Author's work
	U5	4704–06	0.4	0.05	0.30	0.52	440	0.35	0.14	130	75	0.7	–		
	U4	4830–32	1.7	0.18	0.56	0.13	452	0.74	0.24	7.6	33	0.6	–		

(continued on next page)

2012). The Sembar Formation was deposited on the western shelf of the Indian Plate (passive margin setting) during the early Cretaceous period, as it drifted northward and entered warmer latitudes (Iqbal and Shah, 1980; Ahmad et al., 2012). The Sembar Formation is Neocomian (Lower Cretaceous) in age, but it could be as old as Late Jurassic, according to Belemnite biostratigraphy (Fatmi, 1977).

The Sembar Formation has been encountered in several wells of the Indus Basin at depths ranging from 750 m to 3500 m, with thickness varying from 50 m to more than 600 m, as reported in the literature (Iqbal and Shah, 1980; Kadri, 1995; Ahmad et al., 2012). In the studied wells, as given in Table 2, the thickness of shale varies from 17 m to 550 m and contains quartz (40%–50%), clay (30%–40%) and calcite (10%–15%) minerals (Ahmad et al., 2012). The shale of Sembar Formation is the source rock for most of the conventional producing reservoirs in the Middle and Lower Indus Basin and has high values of TOC (2%–10%) and Ro (0.85–1.50%) (Haider et al., 2012). The published geochemical data acquired using well cuttings samples of studied wells (as

given in Table 3) shows the S1 range between 1.79 to 10.16 mg HC/g rock and S2 lie in the range between 2.65–33.91 mg HC/g rock which indicates good to very good and fair to very good quality source rock, respectively. Van Krevelen diagram and S2-TOC (Fig. 4a and c, respectively) plots show that the Sembar Shale contains Type-II and III Kerogen (mixed type) and has the potential to produce oil and gas. On Tmax-HI plot (Fig. 4b), some data points are in the dry gas window, which still needs to be confirmed through more samples from other wells. The Sembar Formation was in the gas generation window at L6-well, as shown in Fig. 6.

3.5. Ranikot Formation

The Paleocene-age Ranikot Formation was deposited in a fluvial environment and is comprised of sandstone with minor shales and siltstones (Hakro and Baig, 2013). The depth and thickness of shale intervals vary from 270 m to 2135 m and, 64 m to 214 m, respectively, in various wells of the MIB and

Table 3 (continued).

	M5	3482	5.0	5.03	16.83	3.84	427	21.86	0.23	77	336	1	Vitrinite 5%, Inertinite 5%	II, Gas prone 25%, Oil prone 70%	
Sembar		3509	2.62	2.85	7.37	4.21	526	5.47	0.52	161	281				
		3518	5.89	10.16	29.75	3.68	422	16.05	0.63	62	505				
		3520	9.48	6.57	33.91	1.93	431	16.05	0.41	20	358				
	L6		3531	2.11	2.37	4.96	3.90	525	7.33	0.32	185	235	1.09	Vitrinite 25%	II/III, wet gas window
			3559	2.09	1.66	4.72	4.88	423	6.38	0.26	233	226	1	–	
			3598	1.86	1.79	2.88	4.19	424	3.65	0.49	225	155			
ML2		3618	4.15	–	5.50	–	531	–	–	214	264				
		3477	1.92	–	4.52	–	–	–	–	–	–				
		3487	1.87	–	2.65	–	–	–	–	–	–				
Lower Goru	L6	2603	1.58	1.12	2.37	4.25	421	3.49	0.32	269	150	–	Vitrinite 10%	III, Gas prone	
		2618	1.77	1.24	4.41	3.28	425	5.65	0.22	185	249				
		2638	1.06	0.57	1.02	2.09	422	1.59	0.36	197	96				
		2653	1.69	0.69	1.26	4.18	438	2.38	0.29	247	75				
		2668	1.60	0.43	1.07	4.55	438	2.03	0.21	284	67				
		2738	1.72	1.36	2.33	5.31	424	3.69	0.37	309	135				
		2758	2.14	1.02	2.95	5.37	428	3.97	0.26	251	138				
		2798	2.00	1.73	2.96	4.97	426	4.69	0.37	249	148				
		2868	2.53	1.65	5.15	4.78	416	6.80	0.24	189	204				
		2898	1.98	0.91	2.13	6.12	429	3.04	0.30	309	108				
		2918	2.10	0.94	2.66	3.22	429	3.60	0.26	153	127				
		2958	2.36	1.47	3.09	3.90	426	4.56	0.32	165	131				
		2983	3.05	2.48	6.14	3.94	426	8.62	0.29	129	201				
		2990	3.24	2.34	8.83	3.36	428	11.17	0.21	104	273				
		3377	2.10	0.96	2.05	4.04	428	3.01	0.31	192	98	–	Vitrinite 5%		
		3399	2.71	1.55	1.76	4.34	416	3.31	0.47	160	65				
		3419	5.22	5.64	17.37	5.38	425	23.01	0.24	103	333				
3452	3.43	3.32	6.07	5.48	428	9.39	0.35	160	177	–	Vitrinite 5%				
L5		2800	1.86	–	1.50	–	440	–	–	–	195				
		2920	2.34	–	1.86	–	442	–	–	–	200				
		3000	1.69	–	2.05	–	450	–	–	–	198				

Robison
et al.
(1999);
Ahmed
et al. 2012;
Siddiqui
et al. (2014)
and Sheikh
and Gao
(2017)

Depth is in meter (m)

Description of standards is taken from “Source Rock Analyzer”-User Manual written by Fujine (2014) for International Ocean Discovery Program

S1 (milligrams of hydrocarbon per gram of rock) indicates free hydrocarbons (gas and oil) in the sample. S1 > 1 mg HC/g rock may be indicative of an oil show.

S2 (milligrams of hydrocarbon per gram of rock) indicates (i) the hydrocarbons result from the cracking of kerogen, (ii) high molecular weight free hydrocarbons that do not vaporize in the S1 peak.

S3 is an indication of the amount of oxygen in the kerogen and is used to calculate the oxygen index. Generally, S3 values >200 mg CO₂/g rock are anomalously high, possibly due to high concentrations of carbonates that break down at temperatures <390 °C and may or may not be valid.

GP genetic potential

PI (production index) is indicative of the conversion of kerogen into free hydrocarbons or, in a general sense, the transformation ratio (Espitalié et al., 1977).

PI < 0.2: immature rocks, PI = 0.3–0.4: typical for samples in the petroleum window, PI > 0.5: may indicate the proximity of migrated hydrocarbons or trapped petroleum

HI (hydrogen index _mg generated HC/g of organic carbon) is normalized hydrocarbon content of a rock sample. Kerogen type information is derived from this value as Type I kerogens are hydrogen-rich, Type III kerogens are hydrogen-poor, Type II kerogens are intermediate between Type I and Type III

OI (oxygen index _mg CO₂/g of organic carbon) is normalized oxygen content of a rock sample. Type III kerogens generally have higher OI than either Type I or II kerogens. However, the hydrogen content is the principal discriminating factor for oil or gas potential. OI may be increased by weathering or mineral matrix interactions, which elevate the S3 value. If TOC is <0.50 wt%, OI may be meaningless. OI correlates with the ratio of O to C, which is high for polysaccharide-rich remains of land plants and inert organic material encountered as background in marine sediments. OI values range from near 0 to ~150. High OI values (>100) are an indicator of continental organic matter or immature organic matter from all sources.

Tmax pyrolysis temperature at which a maximum yield of generated hydrocarbons occurs. Tmax increases with increasing maturation and indicates the stage of maturation of the organic matter. At low S2 peaks the Tmax values are affected by low organic matter content. Also, organic-lean clayey sediments with S2 values as high as 2.00 mg HC/g rock may have unreliable Tmax values. Tmax may be affected by the presence of heavy free hydrocarbons in the S2 peak, which may cause Tmax to be anomalously low (<400 °C). Also, Tmax may be affected by reworked organic matter or salt ionization, which may cause Tmax to be anomalously high (>550 °C). Tmax values and true Tmax temperatures vary with the temperature programming rate and are useful for approximating kinetic values. Tmax is a calibrated temperature and does not represent the true(absolute) temperature.

LIB that were studied for this work. The values of TOC (2%–3%) and Ro (0.85%–1%) from outcrop samples indicate that shales of the Ranikot Formation are organic-rich and thermally mature with type III Kerogen (Hakro and Baig, 2013). The shale intervals contain quartz (60%–70%), clay (10%–30%), and calcite (5%–10%) in outcrop samples (Hakro and Baig, 2013). There is no published geochemical data for this formation, so the shales of Ranikot cannot be interpreted based on outcrop data only. However, the high shale gas reserves have been estimated by US EIA (2015).

3.6. Lower Goru Formation

The Lower Goru Formation is of early Cretaceous age, and shales of this formation were deposited in pro-deltaic to outer shelf environment. Its depth varies from 2250 m to 3650 m, and

the thickness of shales in this formation range from 198 m to 795 m in the LIB (Siddiqui et al., 2014, Author’s work). The Lower Goru shale has favorable values of TOC (1–1.5%) and Ro (2%–3%) and contains quartz (40%–50%), clay (40%–45%) and calcite (5%–10%) (Siddiqui et al., 2014; Haider et al., 2012). The values of S1 (0.57 to 5.64 mg HC/g rock) and S2 (1.02–17.37 mg HC/g rock) indicate fair to good and poor to very good quality kerogen, respectively. Van Krevlen diagram and S2 -TOC (Fig. 4a and c, respectively) plots show that the Goru Shale contains Type-II and III Kerogen and has the potential to produce both oil and gas. Lower Goru is typically typing II with some terrigenous input. The Tmax-HI plot shows the kerogen is thermally mature in L5-well.

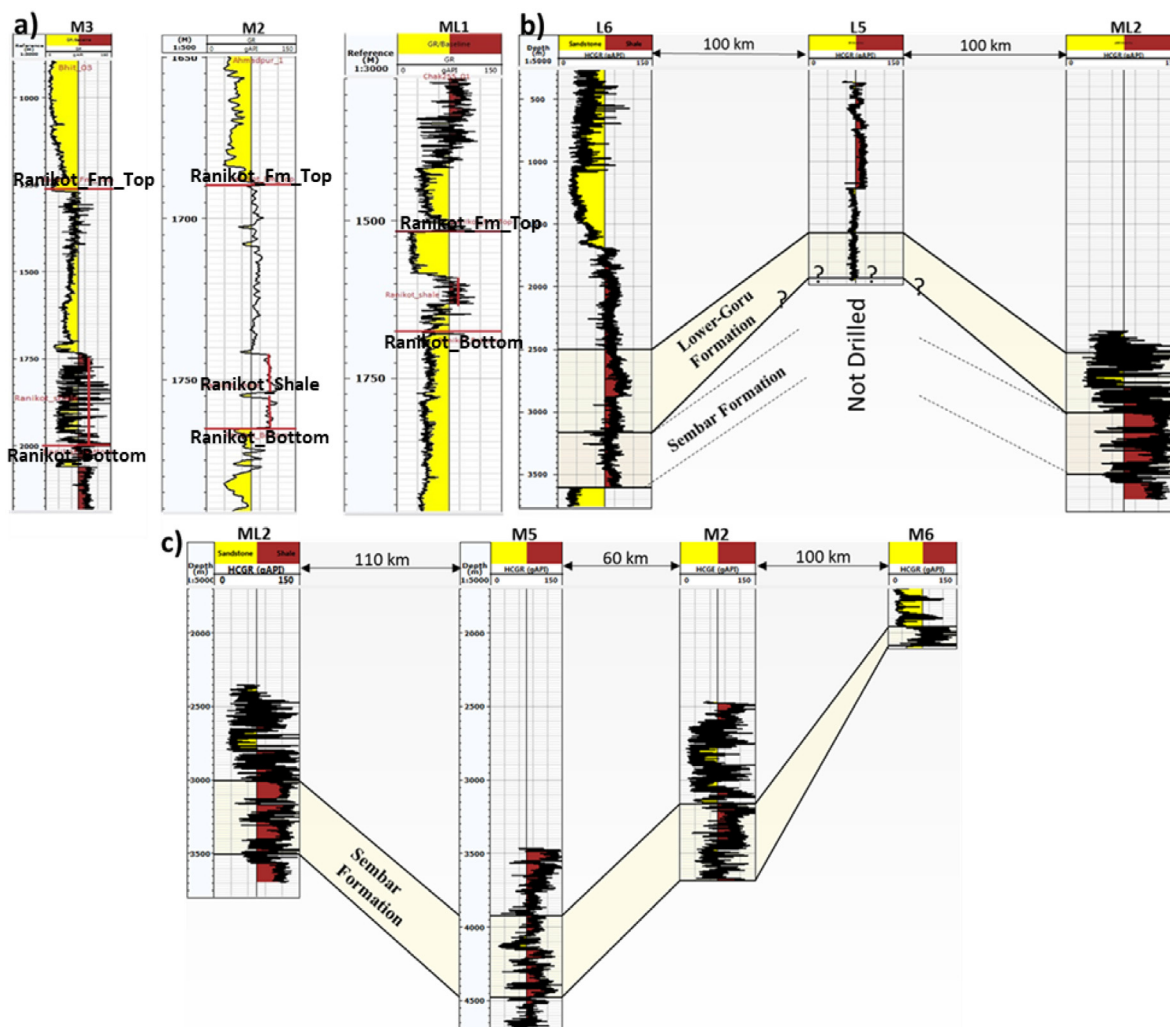


Fig. 3. Wells Correlation based on computed gamma-ray log (CGR and HCGR) for (a) Ranikot, (b) Lower Goru and Sembar and (c) Sembar Formations (see Fig. 1 for wells location) (modified after Sohail, 2020).

4. Producing shale gas plays in the North America

North American shale gas production has increased rapidly in recent decades, with the United States leading the way as the largest producer, followed by Canada in second place. The US shale gas production in 2018 was about 22.3 trillion cubic feet (Tcf) (*online source*), indicating the achievement of large-scale commercial exploitation of shale gas. We will discuss some important shale plays in North America as the following: -

The Marcellus shale produces mostly dry gas, whereas the majority of the other shale plays produce oil or gas liquids. The Barnett shale play, located in Texas, is of Lower Carboniferous age and spans 5000 square miles. It is ranked as the top natural gas onshore play in the United States, as well as the first producing play, due to its shallow depth (1980 to 2600 m). The Haynesville play, which is located in Louisiana, Arkansas, and Texas, is of lower Jurassic age and produces significant natural gas and oil from depth of 3200 to 4100 m. The Eagle Ford Shale Play, which is characterized by favorable brittleness conditions for fracking, produces a large amount of oil and natural gas in southern Texas. The Devonian and Mississippian New Albany Shale is comprised of organically rich brown, black, and green shales. New Albany shale play, located in the Illinois Basin, produces primarily natural gas associated with crude oil. The Antrim Shale, of Upper Devonian age, is composed of brown to black

shales and is found in Michigan, Ohio, Indiana, and Wisconsin, where it is being used for natural gas production. The Fayetteville Shale play in Arkansas and Oklahoma is named after the city of Fayetteville, Arkansas, and it produces natural gas from Mississippian age shales. A sequence of Lower Triassic shales known as the Montney shale play is located in northeast British Columbia and produces both gas and oil. The Duvernay shale play, located in the Western Canadian Sedimentary Basin, is one of Canada's largest shale gas plays, with Frasnian age shales. Crude and liquids are produced in West-Central Oklahoma from the deep (11,500 to 14,500 ft) Anadarko-Woodford Play, which is located in the Anadarko Basin. The Bakken Shale Play in Montana and North Dakota is regarded as one of the most significant oil discoveries, with million barrels of oil produced per day. Deep stacked formations (11,000 to 15,000 ft) in Texas and Oklahoma are producing natural gas and crude oil. The Niobrara Shale Play is a major natural gas and oil producer in South Dakota, Colorado, Nebraska, and Wyoming, with a depth of approximately 6200 ft. The Permian shale plays, located in Western Texas, are one of the largest shale plays in terms of natural gas and oil production. The eight most active shale gas plays, as shown in Table 4, were selected for analog plots with Pakistani shales. Other shale gas plays in North America, as listed in the Appendix, are also used as a basis for comparison later in this paper (discussion section). The selected shales of the USA are producing commercial quantities

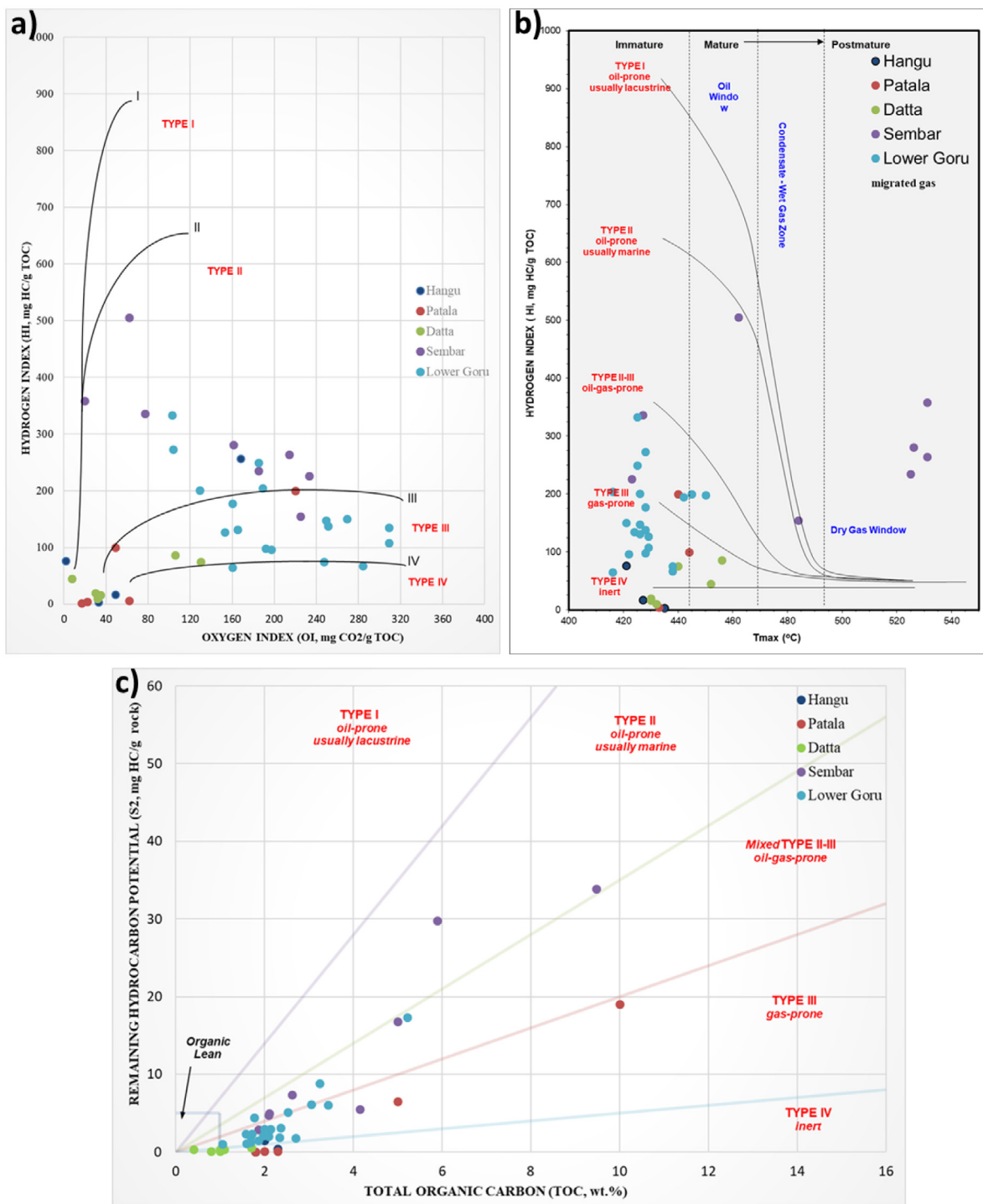


Fig. 4. Kerogen types based on (a) OI and HI cross plot, (b) Kerogen type and maturity, (c) TOC and S2 (data sources are given in Table 3) (modified and reinterpreted after Sohail, 2020).

of natural gas even though all shales exhibit wide ranges of geological and geochemical parameters (Curtis, 2002). Thermogenic and Biogenic gas components are present in most of USA shale gas systems, however in some shales, biogenic gas is dominant (e.g., Antrim and New Albany shale are an example of dual gas components, and Barnett Shale contains thermogenic gas only) (Curtis, 2002).

5. Comparison between selected North American and Pakistani shales

In the following section, various geological and geochemical parameters of Pakistani shales are plotted and compared against those of North American shales, as a means of putting the shale gas potential of Pakistani shales in context.

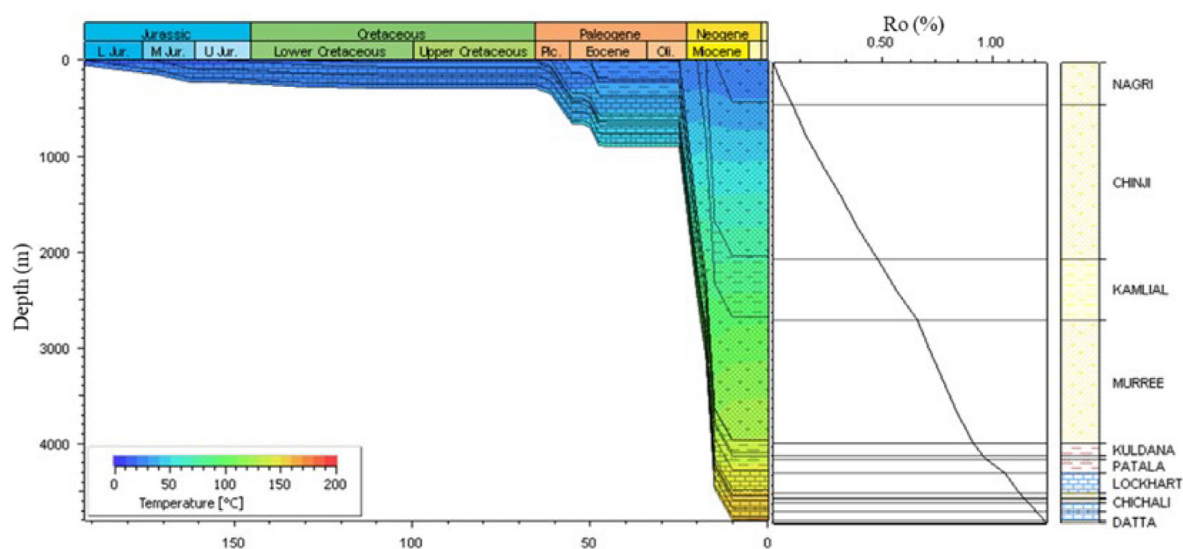


Fig. 5. Burial and Thermal History, and vitrinite reflectance plot of well U1, shows the Datta Formation entered the gas window during Miocene.

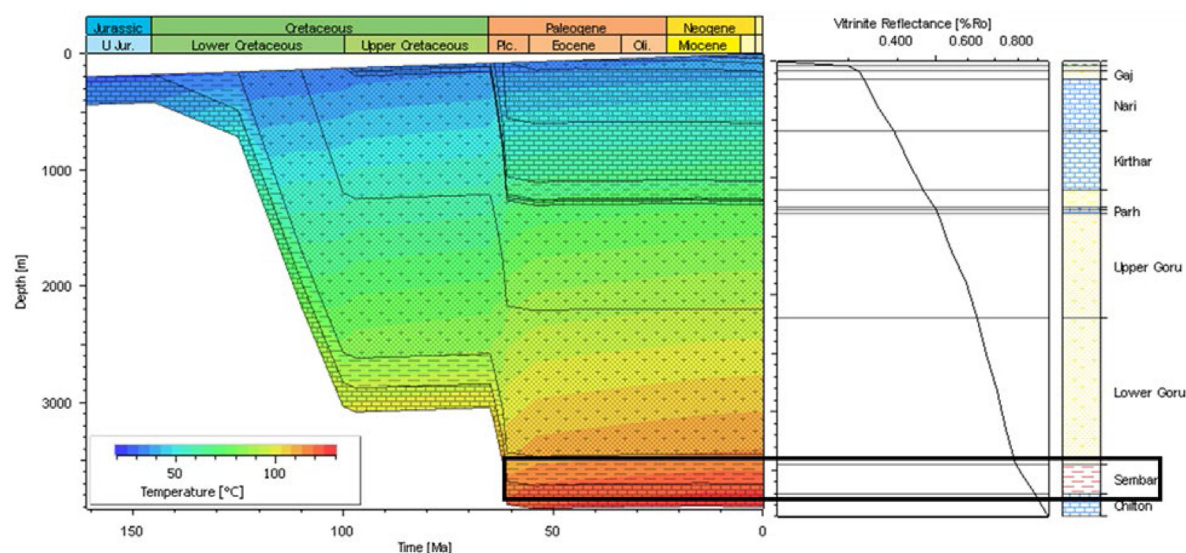


Fig. 6. Burial and Thermal History and vitrinite reflectance plot of well L6, shows the hydrocarbon zone for Sembar Formation at present.

Table 4

Production rates for selected shale gas plays of North America (modified after Sohail, 2020).

Online source: Kennedy et al. (2016).

Shale gas play	Production (bcm/day)
Haynesville	0.19–0.22
Barnett	0.13–0.16
New Albany	0.00019–0.0002
Antrim	0.03–0.05
Eagle Ford	0.15–0.20
Fayetteville	0.36–0.45
Montney	0.01–0.06
Duvernay	0.00005–0.0001

bcm: billion cubic meter.

5.1. Tectonics and depositional environment

Tectonic events of the Mesozoic and Cenozoic eras played important roles in the deposition of Pakistani shales (Fig. 7). In contrast, most of the North American shale gas reservoirs (except

the Haynesville and Eagle Ford shale of the Mesozoic era) were deposited in the Paleozoic era.

North American shales were deposited in flooded foreland basins along collisional margins during the Paleozoic era, and semi-restricted basins along an overall ramp-type setting of a rifted margin during the Mesozoic era (Eoff, 2013; Goldhammer, 1998). Tectonic activities during deposition of Upper Jurassic Haynesville Formation, confined (re)cycling of organic materials to relatively closed systems, which promoted uncommonly thick accumulations of organic matter (Eoff, 2013). The Haynesville shale-gas play deposited in shallow Jurassic strata known as the Sabine Uplift, as well as on the western side of the North Louisiana Salt Basin. The tectonic events relevant to the basement created a series of structural high and low blocks before salt deposition influenced the deposition of younger Jurassic rocks. Later Cretaceous and Cenozoic structural movements may have affected heat flow, burial history, and hence, maturation of the organic section (Hammes et al., 2011). The Indus Basin was located on the passive continental margin of the Indian Plate during the Mesozoic era, and Pakistani shales were deposited under

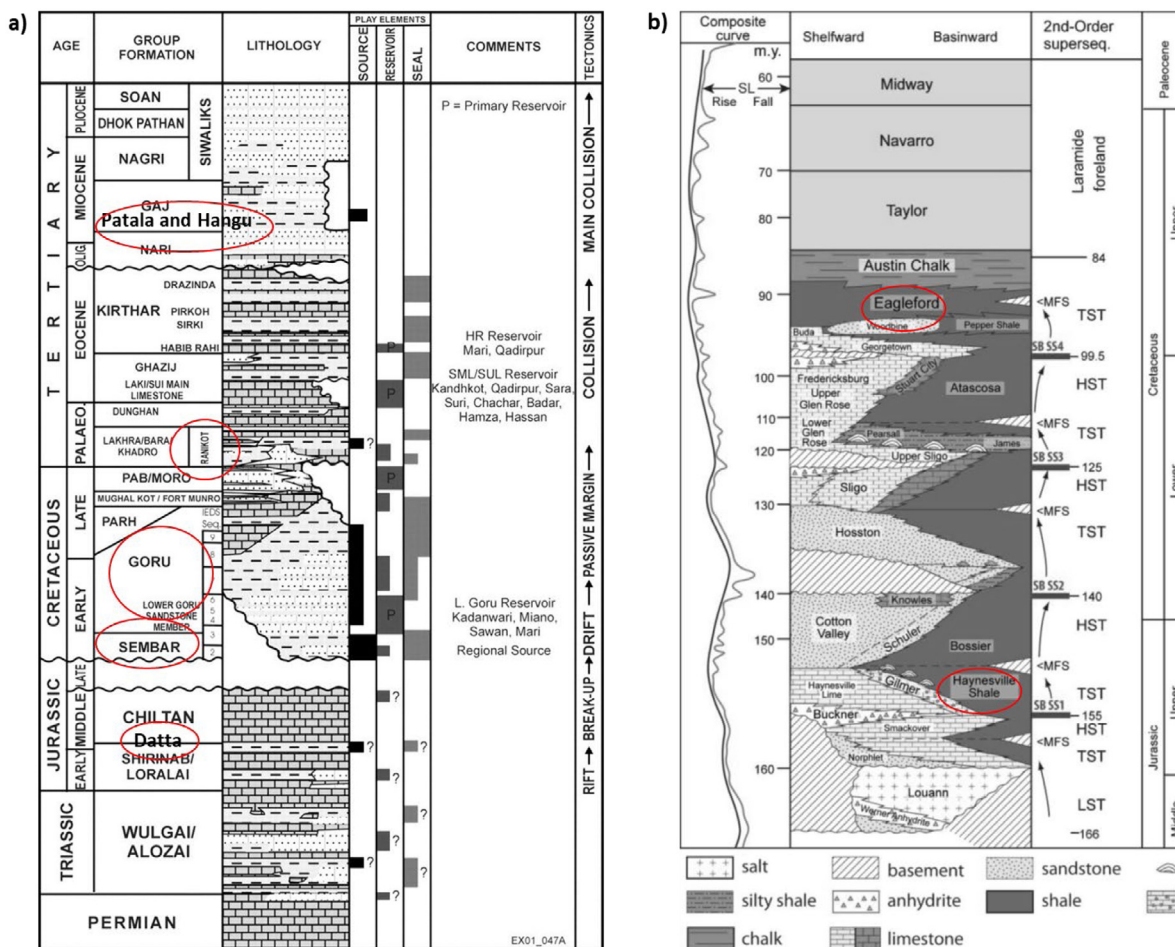


Fig. 7. Tectono-stratigraphy of Pakistani (a) and North American (b) shales (modified after Kadri, 1995; Hammes et al., 2011).

Table 5

Depositional environment of Pakistani and North America shales (see Appendix for details).

Deposition environment	Pakistani shales	North America shales
Shallow marine	Patala, Hangu, Ranikot, Lower Goru, Sembar, Datta,	Haynesville, Devonian, Montney
Deep marine		Barnett, New Albany, Antrim, Eagle Ford, Fayetteville, Duvernay

significant sea-level changes (Kadri, 1995; Khan, 2012). The separation of Eastern Gondwanaland (India–Antarctica–Australia) from Western Gondwanaland (Africa–South America) in the Mesozoic created shallow seas where Pakistani shales of Cretaceous age (e.g., Goru and Sembar) were deposited (Kadri, 1995). In the Tertiary period, movement of the Indian plate accelerated (16 cm/year), and it collided with the Eurasian plate in the north; shales were deposited in different phases of transgression and regression cycles (Kadri, 1995). Geochemical composition of most of shales in Upper and Lower Indus Basin indicates that these are siliceous/argillaceous and contain high organic carbon (Kadri, 1995; Abbasi et al., 2014; Awan et al., 2021).

The studied shales of Pakistan were deposited in shallow marine, and most of North America shales were deposited in deep marine except Haynesville, Devonian and Montney, as given in Table 5.

5.2. Depth and thickness

The burial depths or geological position of the Pakistani shales are generally comparable to or slightly higher than the North American shales, as shown in Fig. 8. At 270 m, the minimum depth of the Ranikot shale is significantly shallower than the other Pakistani shales, which range from 750 to 3600 m minimum depth. The minimum depth of the Ranikot shale is higher than Antrim and New Albany, but lower than the rest (which range from 305 to 3200 m). Maximum depths of the Pakistani shales range from 3500 to 4500 m, compared to North American shales, which vary from 610 to 4268 m. Except for the Sembar shale (minimum and maximum cumulative thicknesses of 17 and 550 m, respectively), the thicknesses of the Pakistani and North American shales fall in similar ranges, as shown in Fig. 9 (4 to 60 m minimum thickness for North American shales compared to 3 to 198 m for Pakistani shales; 21 to 305 m maximum thickness for North American shales compared to 30 to 305 m for Pakistani shales). The minimum thickness (total shale thickness encountered in a single well for a particular formation) of Pakistani shales (<10 m for Datta, Hangu and Patala, as shown in Fig. 9) is comparable to Fayetteville shales of North America. The high maximum accumulative thickness of Lower Goru and Sembar shales is comparable to Barnett, Haynesville, Eagle Ford, Montney shales.

5.3. Mineralogy

According to the ternary plots, shown in Fig. 10a and b, all of the Pakistani shales except the Ranikot and Hangu shales

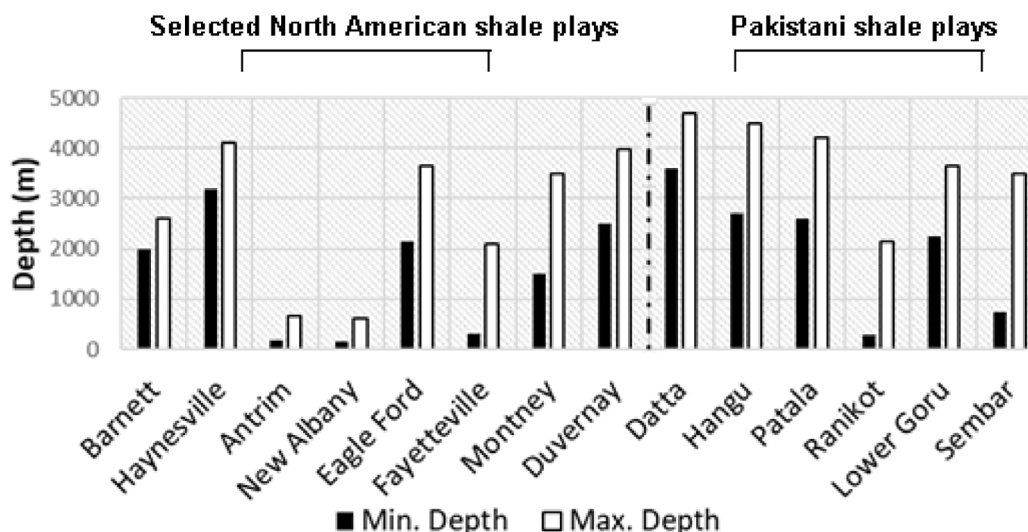


Fig. 8. Depths of selected North American and Pakistani shales (Data sources are given in Appendix).

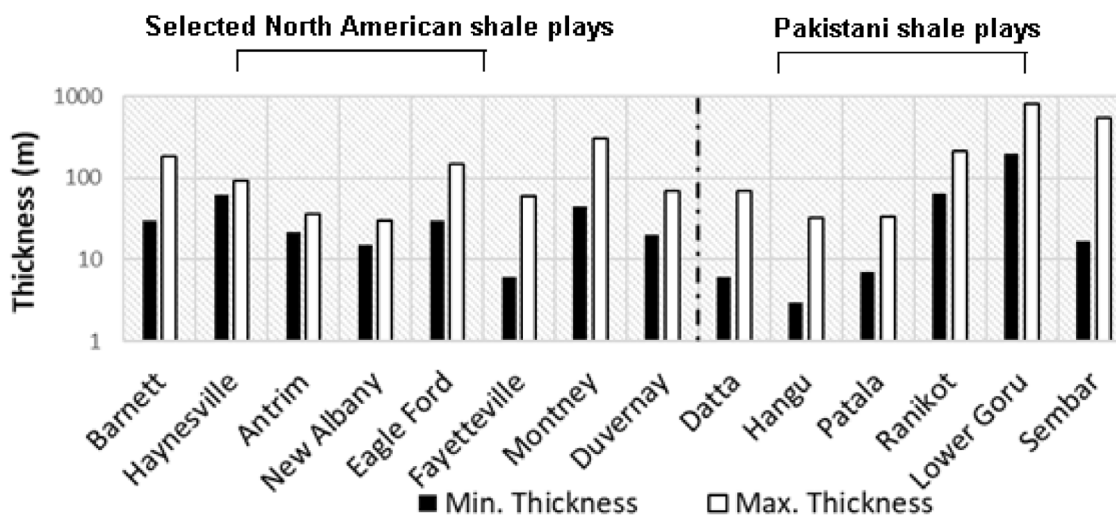


Fig. 9. Thicknesses (single and cumulative thicknesses) of selected North American and Pakistani shales (see Appendix).

have terrigenous quartz contents in the 40% to 50% range (approximately), which is similar to most of the North American shales. North American shales falling below this range are the Haynesville, Duvernay, New Albany (partially) and Eagle Ford. Of these, the latter (Eagle Ford) stands apart from all of the shales studied based on its high calcite content (63% to 73%). The Ranikot and Hangu shales have the highest quartz contents (62% to 75%) of all the shales studied. Pakistani shales that are closest to multiple North American shales in terms of mineralogy are the Sembar (similar to Antrim, New Albany, and Barnett) and the Datta (similar to Montney, Fayetteville and Antrim).

5.4. TOC, Ro, Kerogen type and quality

The content of TOC is an important parameter for the evaluation of source rocks because it reflects the abundance of organic matter. To some extent, it is also used to predict the oxidation–reduction conditions of the water body in which the shale was deposited because the preservation potential of organic matter can be high in a strong anaerobic sedimentary environment. Because the quality and potential of unconventional plays are typically associated with higher TOC values, it is critical in shale gas evaluation. As shown in Fig. 11, minimum TOC for North

American shales is 0.4% to 4% compared to 0.5% to 2% for Pakistani shales; maximum TOC for North American shales is 4% to 25% compared to 2% to 10% for Pakistani shales. The high maximum TOC of the Hangu and Sembar shales (10%) is comparable to the New Albany, Antrim and Duvernay shales. The maximum TOC values for the Ranikot (3%), Lower Goru (1.5%) and Datta (2%) shales are lower than all North American shales. The TOC of Patala Shale (~5%–10%) is comparable to Fayetteville and Eagle Ford shales.

As shown in Fig. 12, minimum Ro for North American shales is 0.35% to 1.29% compared to 0.5% to 2% for Pakistani shales; maximum Ro for North American shales is 1.2% to 4% compared to 1% to 3% for Pakistani shales. Although only one of the top four maximum Ro values (Fayetteville, Lower Goru, Duvernay, and Montney) is associated with a Pakistani shale, overall there is little that differentiates the North American and Pakistani shales regarding Ro values.

5.5. Porosity

As shown in Fig. 13, minimum total porosity for North American shales is 2% to 10% compared to 5% to 10% for Pakistani shales; maximum porosity for North American shales is 5% to

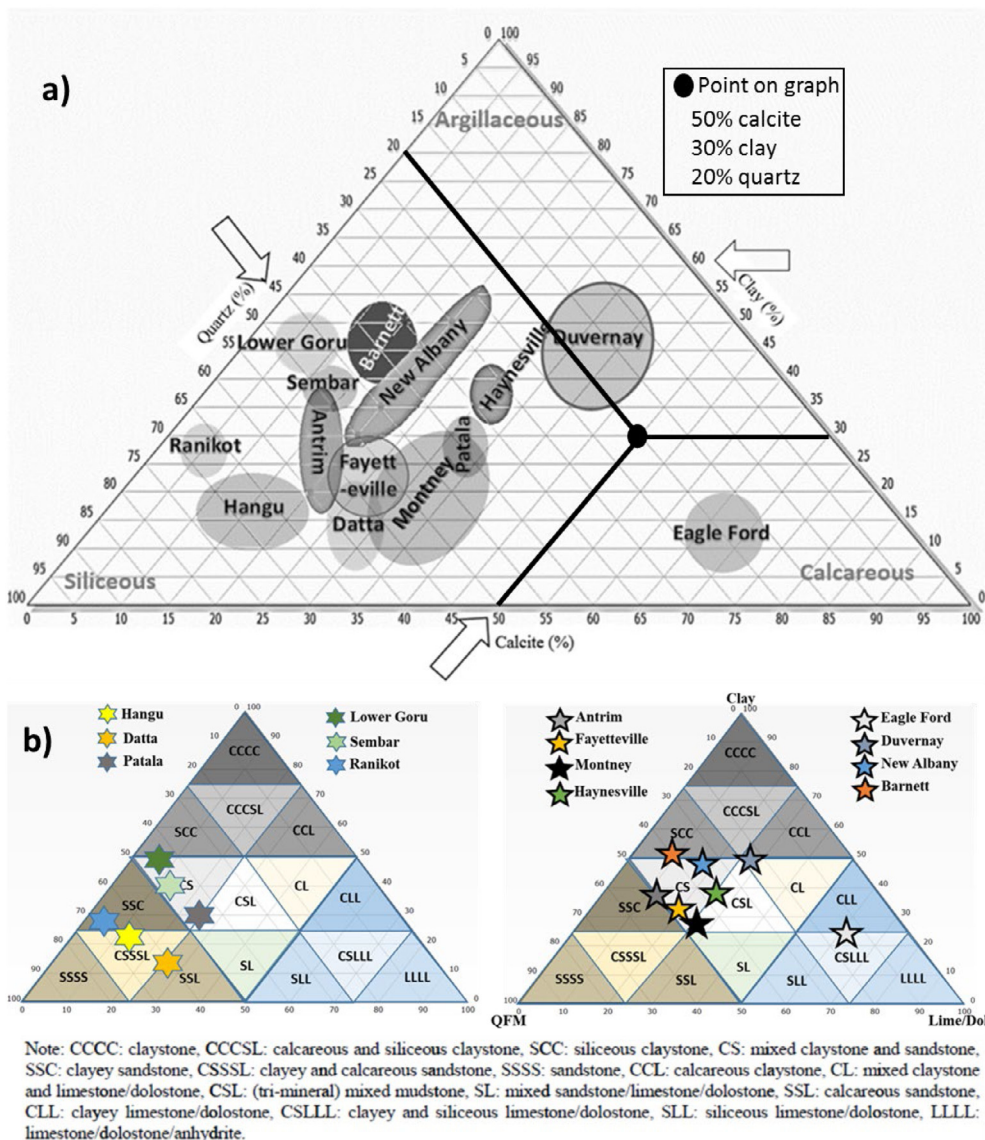


Fig. 10. Ternary plots showing mineralogy of selected North American and Pakistani shales based on (a) published data (source of data is given in the Appendix), and (b) data from a single well (modified after Ma et al., 2016; Sohail, 2020).

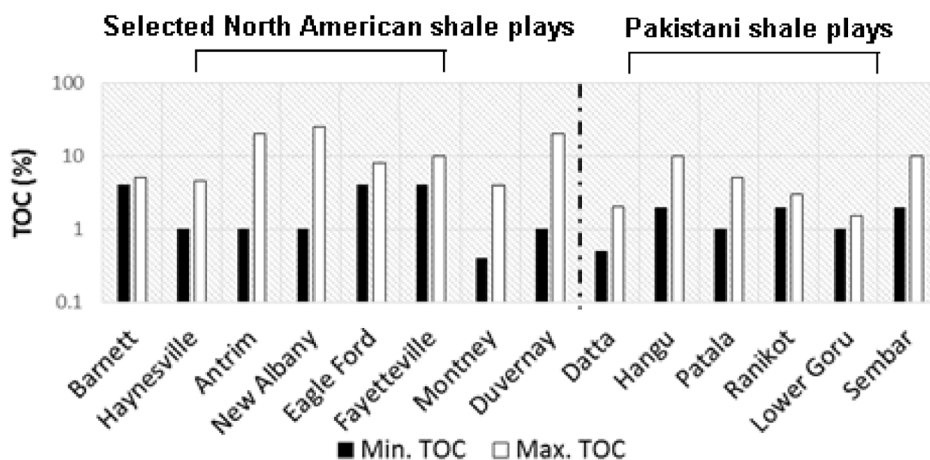


Fig. 11. Total Organic Carbon (TOC) Contents of selected North American and Pakistani shales (see Appendix).

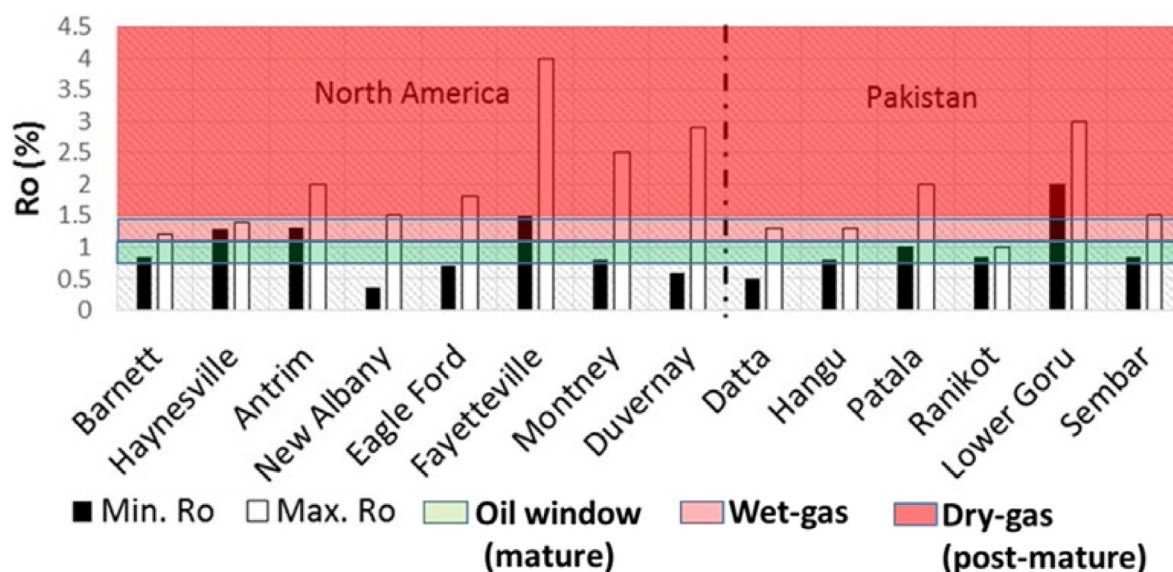


Fig. 12. Vitrinite Reflectance (Ro) values of selected North American and Pakistani shales (see Appendix).

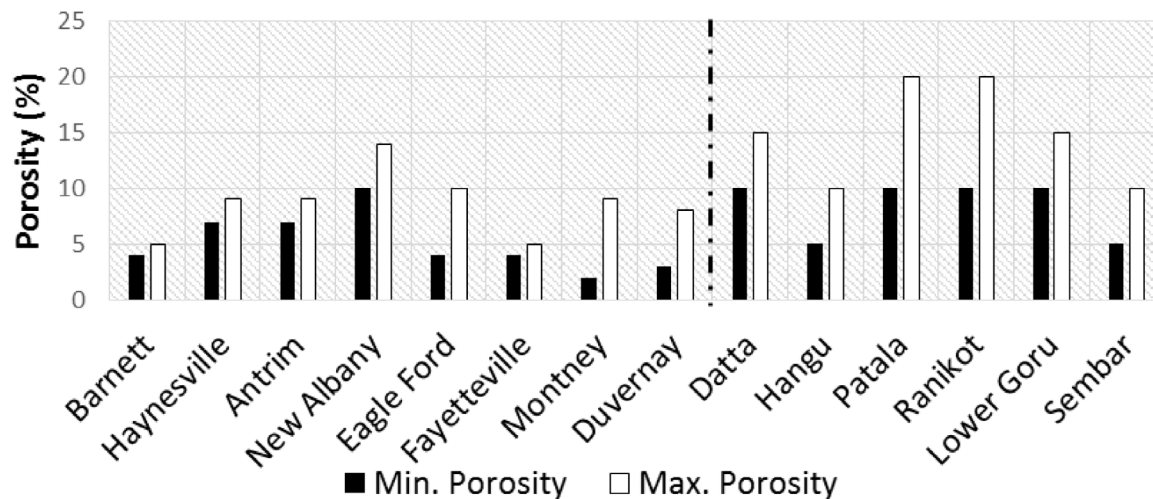


Fig. 13. Porosities of selected North American and Pakistani shales (see Appendix).

14% compared to 10% to 20% for Pakistani shales. Overall, the North American and Pakistani shales are similar in terms of total porosity; as compiled in this study, some Pakistani shales (notably Patala and Ranikot) have higher porosities than North American shales, though it also appears that porosities of Pakistani shales are known with a less degree of precision. In most of the literature, the porosity of Pakistani shales was estimated from porosity logs (e.g., density, neutron and sonic logs). The log-based porosity seemed to be not corrected for shale zones and seems to be overestimated. As a result, petrophysical measurements on the studied Pakistani shales are recommended in order to obtain precise petrophysical parameters of these important source rocks and potential shale plays.

5.6. Methane adsorption in unconventional source rocks

Since there are no field tests for Pakistani shales, we have tried to make acceptable estimates that can be fit with Pakistani shales based on mineralogy and geochemical characteristics. Unconventional source rocks are unlike conventional rocks in terms of storage capacity (Radwan et al., 2022). Gas is mostly stored as free gas in conventional source rocks (Radwan et al., 2022). In

the case of unconventional source rocks, adsorbed gas represents a considerable amount of the initial gas in place and hence controls the gas reserves and gas productivity from unconventional reservoirs (Mahmoud, 2019; Radwan et al., 2022).

Gas adsorption is controlled by several factors that can be listed as follows (Mahmoud, 2019; Mahmoud et al., 2019a,b, 2020):

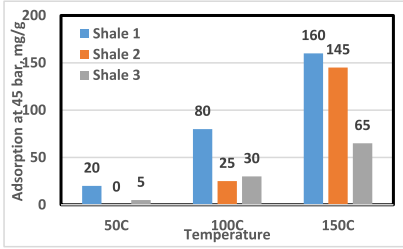
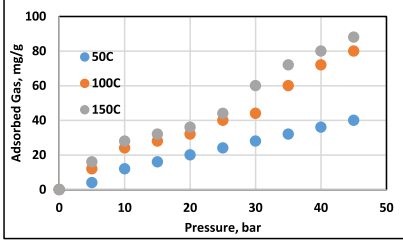
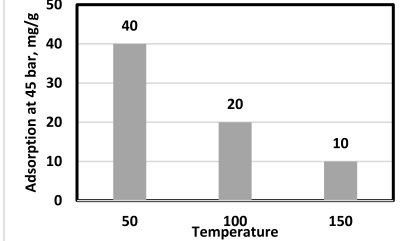
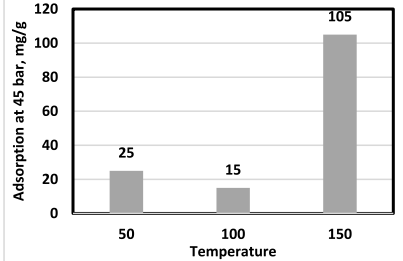
1. Reservoir pressure
2. Reservoir temperature
3. Reservoir rock porosity
4. Rock mineralogy
5. Kerogen content
6. Kerogen maturity

Clay content and type also affect the gas adsorption in shale source rocks at different reservoir conditions (Hamza et al., 2021).

The Table 6 summarizes methane adsorption in different shale source rocks and pure minerals as well.

Based on the results summarized in the previous table, one can conclude that carbonate rocks have less affinity to methane adsorption compared to sandstone rocks. Previous work as reported in the table showed that the methane adsorption decreases with

Table 6
Methane adsorption in different rocks.

Description	Methane adsorption at 45 bar	Reference																
<p>Shale 1 consists of 39% clays, 31% quartz, 10% pyrite, 2% carbonate and 18% feldspar. Total organic carbon 3 wt%. T_{max} is 419 °C which indicates immature shale</p> <p>Shale 2 consists of 54% clays, 24% quartz, 11% pyrite, 3% carbonate and 8% feldspar. Total organic carbon 6 wt%. T_{max} is 417 °C which indicates immature shale</p> <p>Shale 3 consists of 38% clays, 36% quartz, 3% pyrite, and 23% feldspar. Total organic carbon 2 wt%. T_{max} is 472 °C which indicates over mature shale</p> <p>Comparison between three silicate-based shale source rocks at different temperatures. Shales 1 and 2 are immature and shale 3 is over mature (ex. Barnett)</p>	 <table border="1"> <caption>Methane adsorption at 45 bar (Shale 1, 2, 3)</caption> <thead> <tr> <th>Temperature (°C)</th> <th>Shale 1 (mg/g)</th> <th>Shale 2 (mg/g)</th> <th>Shale 3 (mg/g)</th> </tr> </thead> <tbody> <tr> <td>50</td> <td>20</td> <td>0</td> <td>5</td> </tr> <tr> <td>100</td> <td>80</td> <td>25</td> <td>30</td> </tr> <tr> <td>150</td> <td>160</td> <td>145</td> <td>65</td> </tr> </tbody> </table>	Temperature (°C)	Shale 1 (mg/g)	Shale 2 (mg/g)	Shale 3 (mg/g)	50	20	0	5	100	80	25	30	150	160	145	65	Mahmoud et al. (2020)
Temperature (°C)	Shale 1 (mg/g)	Shale 2 (mg/g)	Shale 3 (mg/g)															
50	20	0	5															
100	80	25	30															
150	160	145	65															
<p>Carbonate-based source rock consists of 90% calcite, 5% quartz, 2% clays, 2% anhydrite, 2% pyrite. Total organic carbon is 11%, T_{max} is 470 °C which indicates over mature shale. (ex. Eagle ford)</p>		Mahmoud et al. (2020)																
<p>Calcite adsorption experiments at 45 bar at different temperatures showed that the adsorption decreases with temperature.</p>	 <table border="1"> <caption>Calcite adsorption at 45 bar</caption> <thead> <tr> <th>Temperature (°C)</th> <th>Adsorption (mg/g)</th> </tr> </thead> <tbody> <tr> <td>50</td> <td>40</td> </tr> <tr> <td>100</td> <td>20</td> </tr> <tr> <td>150</td> <td>10</td> </tr> </tbody> </table>	Temperature (°C)	Adsorption (mg/g)	50	40	100	20	150	10	Eliebid et al. (2018)								
Temperature (°C)	Adsorption (mg/g)																	
50	40																	
100	20																	
150	10																	
<p>Kentucky sandstone with 14 wt% clays showed different adsorption behavior at different temperatures. This can be attributed to opening new pores in the clays after heating to 150C.</p>	 <table border="1"> <caption>Adsorption at 45 bar (Kentucky sandstone)</caption> <thead> <tr> <th>Temperature (°C)</th> <th>Adsorption (mg/g)</th> </tr> </thead> <tbody> <tr> <td>50</td> <td>25</td> </tr> <tr> <td>100</td> <td>15</td> </tr> <tr> <td>150</td> <td>105</td> </tr> </tbody> </table>	Temperature (°C)	Adsorption (mg/g)	50	25	100	15	150	105	Hamza et al. (2021)								
Temperature (°C)	Adsorption (mg/g)																	
50	25																	
100	15																	
150	105																	

increasing the temperature in the case of carbonate rocks and pure sandstone rocks (without clay minerals), Eliebid et al. (2018) and Hamza et al. (2021). In the case of sandstone rocks with clays, the adsorption first decreases with increasing temperature and until reaches a critical temperature that can create more pores and change the clay structure and this will cause adsorption to increase again, this was reported in several studies for different sandstone rocks. Sandstone rocks usually consists of clay and this will make the adsorption behavior deviates from the trend.

Unconventional source rocks have higher affinity and higher adsorption capacity to methane compared to conventional rocks. This can be attributed to the existence of the organic materials (Mahmoud et al., 2020). The maturity of organic materials plays a very important role in methane adsorption as shown in the previous table, immature shales will have higher adsorption capacity compared to mature and over mature shale at high temperature. Overmature shale does not have high affinity to adsorb methane compared to the immature ones. Based on the mineralogical composition of the Pakistani shales, it is dominant siliciclastics

based shales (Fig. 10), so their adsorption analog is the Barnett shales.

6. Discussion

The data for North American shales suggest that geological age, depositional environment, depth nor thickness of shale serve as unique indicators of shale gas potential; both old (Devonian) and young (Miocene), deep marine and deltaic, deep (4268 m) and shallow (152 m), thick (915 m) and thin (6 m) shales are successful gas producers (see Appendix for details). Hill and Nelson (2000) considered the favorable shale gas accumulation condition should have thickness more than 30 m. Zhang et al. (2018) evaluated 15 m as a minimum accumulative thickness of shale to accumulate a commercial quantity of gas. In contrast, the minimum effective thickness of a gas generation shale in North America (Fayetteville Shale) is 6 m (Arthur et al., 2008). Some companies in North America reported the minimum favorable net thickness of 20 m (See Appendix). As such, it is necessary to

Table A.1
Data for North American and Pakistani Shales (modified after Sohail, 2020)

Region	Formation	Age	Depositional environment	Depth (m)	Shale thickness (m)	TOC %	Ro %	Mineralogy			ϕ %	K millidarcy	Poisson's ratio fraction	Young's modulus GPa	Remarks
								Quartz	Clay	Calcite					
USA	Barnett	Late Mississippian ¹	Deep marine ^{2,3} (Intrabasinal)	1980–2590 ¹	30–185 ¹	4–5 ¹	1.3–2.1 ¹	35–50 ¹	20–40 ¹	10–15 ¹	4–8 ¹	0.01–0.10 ²	0.15–0.35 ⁴	20–80 ⁴	Brittle ¹
	Haynesville	Upper Jurassic ¹	shallow marine ⁶	3200–4100 ¹	60–90 ¹	1–4.5 ¹	1.29–1.39 ¹	25–45 ¹	30–45 ¹	15–40 ¹	8–9 ¹	0.0056 ⁵	0.12–0.40 ⁴	20–80 ⁴	Ductile ¹
	Antrim	Upper Devonian ⁸	Deep marine ¹⁸	180–670 ⁷	21–70 ⁷	1–20 ⁷	1.3–2.0 ⁸	50–60 ⁹	20–35 ⁹ (illite) 5–10 ⁹ (Kaol.)	–	9 ¹⁰	0.011–0.22 ¹¹	0.20–0.25 ¹²	15–53 ¹²	Brittle ⁹
	New Albany	U.Devonian/L. Mississippian ⁸	Deep Marine ¹⁷ (anoxic)	152–610 ⁷	15–30 ⁷	1–25 ⁷	0.35–1.50 ⁸	25–50 ¹⁴	30–55 ¹⁴ (illite)	Variable ¹⁴	10–14 ⁷	0.017–4 ¹⁵	0.20–0.25 ¹⁶	25–30 ¹⁶	Brittle ¹⁶
	Marcellous	Devonian ¹	Shallow marine, Intrabasinal ²¹	1200–2600 ¹	15–60 ¹	2–8 ¹	1.3–2.4 ¹	10–60 ¹	10–35 ¹	3–50 ¹	4–8 ¹	0.02–0.06 ¹⁹	0.10–0.26 ²⁰	13–28 ²⁰	Brittle ¹
	Fayetteville	Late Mississippian ¹	Marine shelf ¹³	305–2100 ¹	6–60 ¹	4–9.8 ¹	1.5–4.0 ¹	20–60 ¹	30–35 ¹³	1–8 ¹³	4–5 ¹	0.0000857–0.0001822	0.209–0.227 ²²	28–30 ²²	Brittle ²²
	Woodford	U.Devonian/L. Mississippian ¹	Marine, Intrabasinal ²⁴	1525–2900 ¹	5–76 ¹	4–8 ¹	1.2–2.8 ¹	50–65 ¹	30–35 ¹	5–10 ¹	5–6 ¹	0.000045 ²³	<0.16 ²⁴	>28 ²⁴	Brittle ²⁴
	Eagle Ford (mixed oil & gas)	Lower Cretaceous ¹	Marine, Intrabasinal ²⁸	2134–3660 ¹	30–145 ¹	4–8 ¹	0.7–1.8 ¹	20–30 ²⁷	0–4 ²⁷	65–75 ²⁷	4–10 ¹	0.0001–0.01 ²⁶	0.15–0.25 ²⁵	14–17 ²⁵	–
	Niobrara (mixed Oil & gas)	Upper Cretaceous ¹	Transgressive marine ²⁹	915–4268 ¹	15–91 ¹	3 ¹	0.5–1.4 ¹	–	5–10 ²⁹	80–90 ²⁹	7–12 ¹	0.01–3 ³⁰	0.18–0.27 ²⁹	42–62 ²⁹	Brittle ²⁹
	Utica (oil and gas)	Middle Ordovician ¹	Transgressive marine ³¹	610–4268 ¹	21–229 ¹	0.3–2.5 ¹	1.1–4.0 ¹	10–20 ³²	10–20 ³²	45–50 ³²	6–12 ¹	0.000001 ³³	0.2–0.25 ³²	17–31 ³²	–
	Wolf camp (oil)	Permian ¹	Deep marine ³⁴	1676–3354 ¹	457–793 ¹	2–6 ¹	0.8 ¹	45–60 ³⁵	30–40 ³⁵	0–10 ³⁵	2–10 ¹	0.00002–0.008 ³⁵	0.15–0.30 ³⁶	30–50 ³⁶	Brittle ¹
	Monterey (oil)	Miocene ¹	Deep marine ⁴⁰	2439–4268 ¹	305–915 ¹	5 ¹	0.6–1 ¹	50–80 ³⁹	5–15 ³⁹	0–10 ³⁹	13–29 ¹	0.001–1 ³⁸	0.09 ³⁷ Dyn.	10–15 ³⁷ Dyn.	Ductile ³⁸
Bakken (oil)	Late Devonian/Early Mississippian ¹	Shallow to deep marine ⁴¹	2927–3170 ¹	12–23 ¹	9+ ¹	0.6–1 ¹	5–85 ⁴²	25–95 ⁴²	10–15 ⁴²	8–12 ¹	0.001–0.01 ⁴²	0.07–0.45 ⁴³ Dyn.	5.9–7.3 ⁴³ Dyn.	Brittle ⁴²	
Canada	Horn River	Middle Devonian ¹	Deep marine ^{44,45}	1982–2744 ¹	38–137 ¹	1–6 ¹	2.2–2.8 ¹	55–85 ⁴⁵	20–30 ⁴⁵	20–30 ⁴⁵	4–8 ¹	1.04 × 10 ^{–10} –1.99 × 10 ^{–7} ⁴⁶	0.18–0.24 ⁴⁶	11–14 ⁴⁶	Brittle ⁴⁶
	Montney (dry and wet gas)	Early Triassic ¹	Deltaic, shallow marine ⁴⁷	1494–3506 ¹	45–305 ¹	0.4–4 ¹	0.8–2.5 ¹	20–45 ⁴⁸	0–5 ⁴⁸	0–5 ⁴⁸	2–9 ¹	0.01–0.5 ⁴⁸	0.15–0.25 ⁴⁹	27–41 ⁴⁹	Brittle ⁴⁹
	Duverny (mixed oil & gas)	Upper Devonian ¹	Deep marine ⁵⁰	2500–3994 ¹	20–70 ¹	1–20 ¹	0.6–2.9 ¹	50–70 ¹	15–30 ¹	10–30 ¹	3–8 ¹	0.000394 ⁵¹	0.20–0.30 ⁵²	35–50 ⁵²	Brittle ⁵¹
Pakistan	Datta	Jurassic ⁵³	Shallow marine ⁵³	3600–4750 ^{55a}	6–70 ^{55a}	0.5–2.5 ^{55a}	0.5–1.3 ^{55a}	>50 ^a	10–20 ^a (Kaoli)	–	10–15 ^{54a}	0.1–1.15 ^a	–	–	Brittle ^{55a}
	Hangu	Early Paleocene ⁵⁵	Shallow marine ⁵⁵	2700–4500 ^a	3–32 ^a	2–10 ⁵⁸	0.81–1.3 ⁵⁸	60–70 ⁵⁹	<20 ⁵⁹	–	5–10 ⁵⁷	1–4 ^a	–	–	–
	Patala	Late Paleocene ⁶²	Shallow marine ⁶²	2600–4200 ^a	7–33 ^a	1–5.0 ⁵⁸	1–2 ⁵⁸	30–40 ⁶²	25–30 ⁶²	0–20 ⁶²	10–20 ^a	–	–	–	–
	Sembar	Lower Cretaceous ⁶⁰	Pro-deltaic, shallow marine ⁶⁰	750–3500 ^a	17–550 ^a	2–10 ⁵⁸	0.85–1.50 ⁵⁸	40–50 ⁶¹	30–40 ⁶¹	10–15 ⁶¹	5–10 ⁶¹	–	–	–	–
	Ranikot	Paleocene ⁶³	Fluviatile, shallow marine ⁶³	270–2135 ^a	64–214 ^a	2–3 ⁵⁸	0.85–1.00 ⁵⁸	60–70 ⁶³	10–30 ⁶³	0–5 ⁶³	10–20 ^a	–	–	–	–
	Lower Goru	Early Cretaceous ⁶⁴	Pro-deltaic to Outer Shelf ⁶⁴	2250–3650 ^{64a}	198–795 ^a	1–1.5 ⁵⁸	2–3 ⁵⁸	40–50 ⁶⁴	40–45 ⁶⁴	5–10 ⁶⁴	10–15 ^a	–	–	–	–

1. Kennedy et al. (2016), 2. Bruner and Smosna (2011), 3. Loucks and Ruppel (2007), 4. Sone and Zoback (2013a,b), 5. Parker et al. (2009), 6. Ewing (2001), 7. Arthur et al. (2008), 8. East et al. (2012), 9. Ruotsala (1980), 10. US EIA (2011), 11. Reeves et al. (1993), 12. Apotria et al. (1994), 13. Roberts (2013), 14. Mastalerz et al. (2014), 15. Zuber et al. (2002), 16. Salehi (2009), 17. Lineback (1968), 18. Kluesendorf et al. (1988), 19. Soeder (2011), 20. Eshkalak et al. (2014), 21. Barrett (2008), 22. McDonald and Wright (2016), 23. Abusleiman et al. (2007), 24. Gupta et al. (2017), 25. Emadi et al. (2014), 26. Walls and Sinclair (2011), 27. Jansen (2014), 28. Hentz and Ruppel (2010), 29. Corapcioglu (2014), 30. Hovey (2011), 31. Carr et al. (2013), 32. Murphy et al. (2013), 33. Osann and Bilgesu (2015), 34. Franseen et al. (2014), 35. Walls and Morcote (2015), 36. Walls et al. (2016), 37. Perry et al. (2014), 38. Ucof (1988), 39. Rivera et al. (2014), 40. Dobson (2014), 41. LeFever (1991), 42. Sarg (2012), 43. Ahmadov (2011), 44. US EIA (Canada) 2015, 45. Harris and Dong (2013), 46. Hall et al. (2011), 47. Edwin (2013), 48. Rokosh et al. (2010), 49. Nadaraju and Elliott (2010), 50. Walter et al. (2016), 51. Dunn et al. (2012), 52. Soltanzadeh et al. (2015), 53. Abbasi et al. (2011), 54. Khalid et al. (2015), 55. Gul et al. (2016), 56. Warwick et al. (1995), 57. Saddique et al. (2016), 58. Haider et al. (2012), 59. Shah et al. (2013), 60. Wandrey et al. (2004), 61. Ahmad et al. (2012), 62. Jalees (2014), 63. Hakro et al. (2014), 64. Saddique et al. (2016).

^aCalculated using wireline logs.

compare multiple factors. The six Pakistani shales studied here were deposited in shallow marine environments under anoxic conditions and are comparable with the Haynesville, Duverny, and Montney shales. Moreover, due to the anoxic conditions, there is a good possibility of organic matter preservation that would support the occurrence of TOC values exceeding the 1% threshold for good shale gas reservoirs (Bratovich and Walls, 2016).

In terms of quantifying and characterizing organic content, total organic carbon (TOC) content and vitrinite reflectance (Ro) are useful parameters. TOC (notably kerogen and bitumen) defines

the capacity to produce and store hydrocarbons within a shale formation (TOC < 1% suggests a poor-quality shale reservoir; TOC > 1% suggests a good shale reservoir) (Bratovich and Walls, 2016). The range of TOC values for the Pakistani shales has considerable overlap with the North American shales, though they are somewhat lower overall. TOC itself does not show the presence or absence of hydrocarbons; it only predicts the kerogen skeleton that contains carbon only and is blind about the hydrogen element. So, shale samples with TOC > 1% are subjected to pyrolysis study to evaluate the hydrocarbon potential. Most gas-bearing North American Shales are dominant in the organic matter of

Type-II (marine), and type of kerogen for Pakistani shales varies a lot due to a different source and deposition environment, as already illustrated in Fig. 4a, b and c. The mixed type of organic matter in Sembar and Lower Goru Shales (especially Type II and III) was formed in the marine environment of deposition with abundant terrigenous organic matter input and have a potential of both oil and gas generation. Samples of Hangu, Patala were extracted from an outcrop and did not preserve in-situ conditions so the results may be less reliable.

There are two types of shale gas reservoirs, thermogenic and biogenic. The biogenic shale gas needs lower values of vitrinite reflectance (e.g., $R_o < 1.1\%$ for Antrim and New Albany shales) compared to thermogenic shale gas (e.g., $R_o > 1.1\%$ for Barnett Shale) (Song et al., 2015). Jarvie et al. (2007) considered the lower R_o in Barnett shale to be 1.1%. The shales are thermally mature with vitrinite reflectance values of 1.1%–1.4%, and in thermally overmature stage there is a possibility of secondary cracking of insitu oil (Tian et al., 2009). $R_o (< 1.1\%)$ low values for Pakistani shales may not relate to biogenic shale gas due to lack of enough data (e.g., missing molecular and isotopic fingerprints to distinguish biogenic and thermogenic gasses). The high R_o values ($R_o > 1.1\%$) with greater burial depth, the Sembar and Lower Goru shales, are the most favorable candidates for shale gas exploration. These Pakistani shales are already known to serve as source rocks for conventional gas reservoirs, which suggest the likely presence of gas in these shales. The retained gas in Sembar Shale is about 103 billion-cubic-ft/acre-ft (0.002 billion cubic meter/m³), which is favorable (Ahmed et al., 2012; Sheikh and Gao, 2017). Most of the literature on Pakistani shales is relevant to source rock evaluation for the conventional reservoir, so it would not be easy to assess the type of shale gas reservoir. Although for Ranikot, Lower Goru and Sembar shales, the researchers (Ahmed et al., 2012; Sheikh and Gao, 2017) have established the thermogenic origin of the gas. The origin of gas in Hangu, Patala and Datta shales is still under debate and needs more data to conclude.

Most of the North American shales are producing gas after stimulation of brittle intervals of shale reservoir, which creates a network of connected fractures. The fracture gradient is reliant on quartz, clay, and calcite contents in shale. Different researchers Sone and Zoback (2013a,b), Rickman (2008) and Wang and Gale (2009) have linked the mineralogy to brittleness index (BI) of shale gas reservoirs and found the positive correlations between brittle minerals (e.g., quartz) and BI. Although the pyrite and calcite are also critical in the calculation of BI, and separate study should be conducted to reveal the impact of these minerals on BI. Most of the Pakistani shales are poor in calcite, and relatively high in clay and quartz minerals, which may be favorable. The presence of clay is beneficial in the sense of gas-absorption capacity (Passey et al., 2010), but the high clay contents make the shale ductile that is not good for hydraulic fracturing (Sondergeld et al., 2010). Sondergeld et al. (2010) suggested that the quartz content of $> 40\%$ and clay content of $< 30\%$ are desirable for a shale gas reservoir. The mineralogy of Pakistani shales is quite variable between wells; still, most of shales (Hangu, Patala, Datta, Ranikot) fall below 30% clay content threshold. The Lower Goru and Sembar shales contain higher clay contents ($> 30\%$) and falling below the Barnett shale on ternary plot, which suggests that these Pakistani shales still be prospective and may present challenges for production.

There are no distinct threshold values for porosity and permeability of a shale gas play. Still, some researchers (e.g., Bratovich and Walls, 2016; Crain, 2016) recommend the study of porosity systems along with mineralogy within organic-rich shales to help in reserve estimates and stimulation design. In a continental shelf and shallow marine environment, the relatively high quartz

content makes the shales more porous as compared to shales from deep marine settings (Kennedy et al., 2016), so the Pakistani shales are expected to match – and in some cases exceed – the porosity of the North America shales. Compared to the North American shales (porosities generally in the 5% to 10% range), the Pakistani shales (particularly Sembar and Lower Goru Shales) have similar or higher values of porosity (up to 15%); this is favorable.

Considering near shale gas plays in China, the Silurian gas plays in China have produced gas (Chen et al., 2015; Xin et al., 2019; Guo et al., 2019; Shu et al., 2020). Therefore, considering the depths, thickness, mineralogy, and porosity, it is recommended to compare the Pakistani six shale with the nearby Chinese gas plays in future work, especially on Silurian gas resources.

7. Conclusion

This review documents the key parameters of North American and Pakistani Shales, a direct comparison of both shales is presented for the assessment of Pakistani Shales as a shale gas candidate. The following conclusions can be drawn from this review:

- All the studied shales of Pakistan qualify an initial criterion for shale gas exploration concerning North America shales, and Sembar and Lower Goru Shales are looking more promising compared to other Pakistani shales.
- The Pakistani shales, particularly Sembar and Lower Goru, compare favorably in terms of depth, thickness, TOC, R_o , and porosity. Relatively high quartz contents in these shales (i.e., approximately 50%) are favorable for hydraulic fracturing.
- Notable is the fact that permeability, Poisson's ratio, and Young's modulus are available for the North America shales, but not for the Pakistani shales. These missing parameters are critical to deciding the economic feasibility of a shale gas reservoir even though shale formation is deeper, thick, thermally mature, organically rich and porous. Once these properties have been measured and compiled, the North American data can be used as a basis for comparison of these properties.

CRedit authorship contribution statement

Ghulam Mohyuddin Sohail: Conceptualization, Methodology, Software, Investigation, Writing – original draft, Reviewing and editing. **Ahmed E. Radwan:** Conceptualization, Methodology, Software, Investigation, Writing – original draft, Reviewing and editing. **Mohamed Mahmoud:** Reviewing and editing.

Declaration of competing interest

The authors declare that they have no known competing financial interests or personal relationships that could have appeared to influence the work reported in this paper.

Acknowledgments

The author acknowledges DGPC (Directorate General of Petroleum Concession) and HDIP (Hydrocarbon Development Institute of Pakistan) for giving wells data and University of Saskatchewan, Canada, and University of Engineering & Technology, Lahore, Pakistan for facilitating this research. I am thankful to Dr. Muhammad Asif (Petroleum Geochemist, Exxon Mobil, Texas, USA) and Dr. Christopher Hawkes (Associate Professor, Department of Civil, Geological and Environment Engineering, University of Saskatchewan) for giving suggestions to improve this manuscript.

Appendix

See Table A.1.

References

- Abbasi, I.A., Haneef, M., Obaid, S., Daud, F., Qureshi, A.W., 2011. Mesozoic deltaic system along the western margin of the Indian plate: Lithofacies and depositional setting of datta formation, north Pakistan. *Arab. J. Geosci.* 5 (3), 471–480. <http://dx.doi.org/10.1007/s12517-010-0276-1>.
- Abbasi, A.H., Mehmood, F., Kamal, M., Naqvi, S., 2014. Shale Oil and Gas: Lifeline for Pakistan. A Report. Sustainable Development Policy Institute, Islamabad, Pakistan, p. 136.
- Abdelghany, W.K., Radwan, A.E., Elkhawaga, M.A., Wood, D., Sen, S., Kassem, A.A., 2021. Geomechanical modeling using the depth-of-damage approach to achieve successful underbalanced drilling in the gulf of sues rift basin. *J. Pet. Sci. Eng.* 202, 108311. <http://dx.doi.org/10.1016/j.petrol.2020.108311>.
- Abousleiman, et al., 2007. Geomechanics Field and Laboratory Characterization of Woodford Shale: The Next Gas Play. SPE Annual Technical Conference and Exhibition SPE 110120.
- Ahmad, N., Javed, M., Kashif, S., Mehmood, N., Arif, F., 2012. Shale Gas Potential of Lower Cretaceous Sembar Formation in Middle and Lower Indus Sub-Basins, Pakistan. Search and Discovery, Retrieved May 7, 2018, from http://www.searchanddiscovery.com/abstracts/pdf/2012/90138papg/abstracts/ndx_ahmad04.pdf.
- Ahmadov, R.S., 2011. Microtextural Elastic and Transport Properties of Source Rocks (Ph.D. thesis). Stanford University, p. 120, (Retrieved 2016, from <http://purl.stanford.edu/bt842hc0861>).
- Apotria, T., Kaiser, C.J., Cain, B.A., 1994. Fracturing and stress history of the devonian antrim shale, Michigan basin. In: Nelson, P.P. and Lanbach, S.E. (Eds.) Proceedings of 1st North American Rock Mechanics Symposium, January 1-3, 8, pp. 809–816.
- Arthur, D.J., Langhus, B., Alleman, D., 2008. An overview of modern shale gas development in the United States, a report all consulting engineers, U.S.A. p. 21.
- Asif, M., 2010. Geochemical Applications of Polycyclic Aromatic Hydrocarbons in Crude Oils and Sediments from Pakistan (Ph.D. thesis). retrieved November 26, 2018, from <http://pr.hec.gov.pk/jspui/bitstream/123456789/303/1/2715.pdf>.
- Awan, R.S., Liu, C., Aadil, N., Yasin, Q., Salaam, A., Hussain, A., Gul, M.A., 2021. Organic geochemical evaluation of cretaceous talhar shale for shale oil and gas potential from lower indus basin, Pakistan. *J. Pet. Sci. Eng.* 200, 108404. <http://dx.doi.org/10.1016/j.petrol.2021.108404>.
- Ayaz, A.S., Haider, A.B., Ismail, K., Smith, M.P., 2012. Unconventional hydrocarbon resource plays in Pakistan: An overview awakening a south east asian sleeping giant-technological solutions to unlock the vast unconventional reserves of Pakistan. In: Proceedings of Geoscience Technology Workshop (GTW) on Unconventional Hydrocarbons, Singapore, March 15-16, pp. 20–45.
- Barrett, R., 2008. The Depositional Setting of the Marcellus Black Shale. Seminar conducted by Independent Oil and Gas Association of West Virginia, pp. 1–4, July 15.
- Bratovich, W.M., Walls, F., 2016. The unconventional basins and plays-north america, the rest of the world and emerging basins. In: U., Ahmed, M.D., Nathan (Eds.), Unconventional Oil and Gas Resources: Exploitation and Development. Baker Hughes, Canada, pp. 8–60.
- Bruner, R., Smosna, R., 2011. A comparative study of the Mississippian Barnett Shale, Fort Worth Basin, and Devonian Marcellus Shale, Appalachian Basin. Technical Report. doi:DOE/ NETL-2011/1478.
- Caineng, Z., Dazhong, D., Yuman, W., Xinjing, L., J. HUA.N.G., Shufang ..., W., Zhen, Q., 2015. Shale gas in China: Characteristics, challenges and prospects (1). *Pet. Explor. Dev.* 42 (6), 753–767.
- Carr, R.T., Wang, G., McClain, T., 2013. Petrophysical Analysis and Sequence Stratigraphy of Utica Shale and Marcellus Shale, Appalachian Basin, USA. International Petroleum Technology Conference, China, pp. 2–12.
- Chalmers, G., Bustin, R., 2008. Lower cretaceous gas shales in northeastern british Columbia, part I: geological controls on methane sorption capacity. *Bull. Can. Pet. Geol.* 56, 1–21. <http://dx.doi.org/10.2113/gscpgbull.56.1.1>.
- Chen, L., Lu, Y., Jiang, S., Li, J., Guo, T., Luo, C., Xing, F., 2015. Sequence stratigraphy and its application in marine shale gas exploration: A case study of the lower silurian longmaxi formation in the jiaoshiba shale gas field and its adjacent area in southeast sichuan basin, SW China. *J. Nat. Gas Sci. Eng.* 27, 410–423.
- Corapcioglu, H., 2014. Fracturing Fluid Effects on Young's Modulus and Embedment in the Niobrara Formation (M.Sc. Thesis). Colorado School of Mines, USA.
- Crain, E.R., 2016. Crain's petrophysical handbook - special cases – gas shales. p. 1, (Retrieved March 30, 2016, from <https://spec2000.net/17-specshgas.htm>).
- Cui, X., Radwan, A.E., 2022. Coupling relationship between current in-situ stress and natural fractures of continental tight sandstone oil reservoirs. *Interpretation* 10 (3), 1–53.
- Curtis, J.B., 2002. Fractured shale-gas systems. *AAPG Bull.* 86. <http://dx.doi.org/10.1306/61eeddbb-173e-11d7-8645000102c1865d>.
- Dobson, P., 2014. Prospective Application of Well Stimulation Technologies in California, Report. California Council on Science and Technology, (Retrieved from <https://ccst.us/publications/2014/2014wst4.pdf>).
- Dunn, L., Schmidt, G., Hammermaster, K., Brown, M., Bernard, R., Wen, E., Befus, R., Gardiner, S., 2012. The Duvernay Formation (Devonian): Sedimentology and Reservoir Characterization of a Shale Gas/Liquids Play in Alberta, Canada. Geo-Convention: Vision, Canada, pp. 1–5.
- East, A.J., Swezey, S.C., Repetski, E.J., Hayba, O.D., 2012. Thermal maturity map of devonian shale in the illinois, Michigan, and appalachian basins of north America. *US Geol. Surv. Bull.* 1–25.
- Edwin, I.E., 2013. Tight Gas Reservoir Characterization in Montney Formation, Northeastern British Columbia, Western Canada (Ph.D. thesis). Department of Earth and Atmospheric Sciences, University of Alberta, Canada.
- Eliebid, M., Mahmoud, M., Shawabkeh, R., Elkhatny, S., Hussein, I.A., 2018. Effect of CO2 adsorption on enhanced natural gas recovery and sequestration in carbonate reservoirs. *J. Nat. Gas Sci. Eng.* 55 (2018), 575–584. <http://dx.doi.org/10.1016/j.jngse.2017.04.019>.
- Emadi, H., Soleiman, M., Samuel, R., Harville, D., Gamadi, T., 2014. Effect of temperature on the compressive strength of eagle ford oil shale rock: An experimental study. In: IADC/SPE Drilling Conference and Exhibition, Texas, USA. pp. 1–9.
- Eoff, D.J., 2013. Shale hydrocarbon reservoirs: Some influences of tectonics and paleogeography during deposition. In: Geology of the Haynesville Gas Shale in East Texas and West Louisiana, Vol. 105. AAPG Memoir, pp. 5–27, (Retrieved 2016, from http://archives.datapages.com/data/specpubs/memoir105/data/5_aapgsp1950005.htm?doi=10.1306%2F13441842M1053597#aff1).
- Eshkalak, O.M., Mohaghegh, D.S., Esmaili, S., 2014. Geomechanical properties of unconventional shale reservoirs. *J. Pet. Eng.* 2, 10–12.
- Ewing, T.E., 2001. Review of late jurassic depositional systems and potential hydrocarbon plays of the northern gulf of Mexico basin. *AAPG Bull.* 85, 85–96.
- Fatmi, A.N., 1977. Mesozoic. In: Ibrahim, S.M. (Ed.), Stratigraphy of Pakistan. Geological Survey of Pakistan.
- Franseen, K.E., Goldstein, H.R., Doveton, J., 2014. Depositional controls on distribution and reservoir character of deep water deposits in the permian wolfcamp, bone spring, and wolfbone plays of the delaware basin. In: Kansas Interdisciplinary Carbonates Consortium Prospectus. pp. 1–25.
- Fujine, K., 2014. Source Rock Analyzer–User Guide. International Ocean Discovery Program, v1.1.
- Goldhammer, R.K., 1998. Second-order accommodation cycles and points of stratigraphic turnaround: Implications for high-resolution sequence stratigraphy and facies architecture of the haynesville and cotton valley lime pinnacle reefs of the east texas salt basin. In: Houston Geological Society Bulletin North American Explorationists Meeting, Houston, Texas, April, 27, pp. 1–2.
- Gul, A.M., Khan, S.M., Sohail, M.G., 2016. Evaluation of shale gas prospect in datta formation, upper indus basin, Pakistan. *J. Pak. Inst. Chem. Eng.* 44 (1), 1–8.
- Guo, X., Qin, Z., Yang, R., Dong, T., He, S., Hao, F., Liu, K., 2019. Comparison of pore systems of clay-rich and silica-rich gas shales in the lower silurian longmaxi formation from the jiaoshiba area in the eastern sichuan basin, China. *Mar. Pet. Geol.* 101, 265–280.
- Gupta, N., Rai, S.C., Sondergeld, H.C., 2013. Petrophysical characterization of the woodford shale. *Petrophysics* 54 (4), 368–382.
- Haider, A.B., Aizad, T., Ayaz, A.S., Shoukry, A., 2012. A Comprehensive Shale Gas Exploitation Sequence for Pakistan and Other Emerging Shale Plays. Society of Petroleum Engineers (SPE) Annual Technical Conference, Islamabad, Pakistan, pp. 1–21.
- Hakro, D.A., Baig, A.M., 2013. Depositional environment of the bara formation, Fort Ranikot Area, Sindh. *Sindh Univ. Res. J. Sci. Ser.* 45 (1), 83–94.
- Hakro, A.A., Baig, A.M., Baqri, R.S., Khokhar, Q., 2014. Clay mineralogy of the bara formation exposed at Ranikot, Lakhra and in the subsurface of thar coalfield, Sindh, Pakistan. *Int. J. Econ. Environ. Geol.* 5 (2), 32–38.
- Hall, D.C., Jennings, D., Miller, R., 2011. Comparison of the Reservoir Properties of the Muskwa (Horn River Formation) with Other North American Gas Shales, A Report. Core Laboratories, Houston, Texas, U.S.A, p. 3.
- Hammes, U., Hamlin, H., Ewing, T., 2011. Geologic analysis of the upper jurassic haynesville shale in east Texas and west Louisiana. *AAPG Bull.* 95 (10), 1643–1666. <http://dx.doi.org/10.1306/02141110128>.
- Hamza, A., Hussein, I., Al-Marri, M., Mahmoud, M., Shawabkeh, R., 2021. Impact of clays on CO2 adsorption and enhanced gas recovery in sandstone reservoirs. *Int. J. Greenh. Gas Control* 106 (2021), 103286. <http://dx.doi.org/10.1016/j.jggc.2021.103286>.
- Hao, F., Zou, H., Lu, Y., 2013. Mechanisms of shale gas storage: Implications for shale gas exploration in China. *AAPG Bull.* 97 (8), 1325–1346.
- Harris, B.N., Dong, T., 2013. Characterizing porosity in the Horn River shale, Northeastern British Columbia. Geoscience Reports, British Columbia Ministry of Natural Gas Development, p. 40.

- Hentz, T.F., Ruppel, S.C., 2010. Regional Lithostratigraphy of the Eagle Ford Shale: Maverick Basin to East Texas Basin. *Transactions of the Gulf Coast Association of Geological Societies, Society of Economic Paleontologists and Mineralogists, Annual Meeting*, pp. 225–337.
- Hill, D.G., Nelson, C.R., 2000. Gas productive fractured shales: An overview and update. *Gas Tips* 6 (3), 4–13. <https://www.semanticscholar.org/paper/Gas-productive-fractured-shales%3B-an-overviewand-DavidCharles/0143440fb1acbbfd007200b799ea6eb74be2810b>.
- Hovey, R., 2011. The Niobrara Shale. A Report. Energy Strategy Partners, U.S.A, p. 37.
2008. <https://geology.com/world/pakistan-satellite-image.shtml>. (Accessed 10 January 2021).
- Iqbal, M.W.A., Shah, S.M.I., 1980. A Guide to the Stratigraphy of Pakistan, Geological Survey of Pakistan Records, Vol. 53. Geological Survey of Pakistan, Quetta, pp. 340–350.
- Jalees, I.M., 2014. Geochemical Segregation of Petroleum Systems of Potwar Basin using GC-MS and Pyrolysis Techniques (Ph.D. thesis). Department of Chemistry, University of Engineering & Technology, Lahore, Pakistan, p. 140.
- Jansen, A.T., 2014. The Effect of Rock Properties on Hydraulic Fracture Conductivity in the Eagle Ford and Fayetteville Shales (M.Sc. Thesis). Texas A & M University, USA, p. 45.
- Jarvie, D.M., 2012. Shale resource systems for oil and gas: Part 1 – shale-gas resource systems. In: Breyer, J.A. (Ed.), *Shale Reservoirs – Giant Resources for the 21st Century*, Vol. 97. AAPG Memoirs, pp. 69–87. <http://dx.doi.org/10.1306/13321446M973489>.
- Jarvie, D.M., Hill, R.J., Ruble, T.E., Pollastro, R.M., 2007. Unconventional shale-gas systems: The mississippian barnett shale of north-central texas as one model for thermogenic shale-gas assessment. *AAPG Bull.* 91 (4), 475–499. <http://dx.doi.org/10.1306/10.1306/12190606068>.
- Kadri, I.B., 1995. Petroleum Geology of Pakistan. Pakistan Petroleum Ltd, Karachi.
- Kazmi, A.H., Abbasi, I.A., 2008. Stratigraphy and Historical Geology of Pakistan. Department & NCE in Geology, University of Peshawar, Pakistan.
- Kennedy, R., Luo, X.L., Kussakra, V., 2016. The unconventional basins and plays-north America, the rest of the world and emerging basins. In: U., Ahmed, M.D., Nathan (Eds.), *Unconventional Oil and Gas Resources: Exploitation and Development*. Baker Hughes, Canada, pp. 2–33.
- Khalid, P., Yasin, Q., Sohail, M.G., Kashif, M., 2015. Integrating core and wireline log data to evaluate porosity of jurassic formations of injra-1 and nuryal-2 wells, western Potowar. *J. Geol. Soc. India* 86, 553–562.
- Khan, S., 2012. Biostratigraphy and Microfacies of the Cretaceous Sediments in the Indus Basin, Pakistan (Ph.D. thesis). The University of Edinburg, UK.
- Kluessendorf, J.J., Mikulic, G.D., Carman, R.M., 1988. Distribution and depositional environments of the westernmost devonian rocks in the Michigan basin, devonian of the world. In: *Proceedings of the 2nd International Symposium on the Devonian System – Memoir 14, Volume I: Regional Syntheses*. pp. 251–263.
- LeFever, J.A., 1991. History of oil production from the bakken formation, north Dakota. In: Hansen, W.B. (Ed.), *Guidebook to Geology and Horizontal Drilling of the Bakken Formation*. Montana Geological Society, pp. 9–17.
- Lineback, J.A., 1968. Subdivisions and depositional environments of new alban shale (devonian-mississippian) in Indiana. *AAPG Bull.* 7, 1290–1302.
- Liu, J., He, Z.L., Liu, X.W., Huo, Z.Z., Guo, P., 2019. Using frequency-dependent AVO inversion to predict the sweet spots of shale gas reservoirs. *Mar. Pet. Geol.* 102, 283–291.
- Loucks, R.C., Ruppel, S.C., 2007. Missipian barnett shale: lithofacies and depositional setting of a deep-water shale-gas succession in the fort worth basin, Texas. *AAPG Bull.* 92, 579–601.
- Ma, Y.Z., Moore, W., Gomez, E., Luneau, B., Kaufman, P., Gурpinar, O., Handwerker, D., 2016. Wireline log signatures of organic matter and lithofacies classifications for shale and tight carbonate reservoirs. *Unconven. Oil Gas Resour. Handb.* 151–171. <http://dx.doi.org/10.1016/b978-0-12-802238-2.00005-5>.
- Mahmoud, M., 2019. Effect of gas adsorption on the estimation of gas in place (GIP) in conventional and unconventional reservoirs. *AJSE* 44 (6), 6205–6214. <http://dx.doi.org/10.1007/s13369-019-03815-9>.
- Mahmoud, M., Eliebid, M., Al-Yousef, H., Kamal, M., Al-Garadi, K., 2019b. Impact of methane adsorption on tight rock permeability measurements using pulse-decay. *Petroleum* 5 (4), 382–387. <http://dx.doi.org/10.1016/j.petlm.2019.01.002>.
- Mahmoud, M., Hmaza, A., Hussein, I.A., Eliebid, M., Kamal, M., Abouelresh, M., Shawabkeh, R., Al-Marri, M., 2020. Carbon dioxide EGR and sequestration in mature and immature shale: adsorption study. *JPSE* 188 (2020), 106923. <http://dx.doi.org/10.1016/j.petrol.2020.106923>.
- Mahmoud, M., Hussein, I.A., Carchini, G., Shawabkeh, R., Eliebid, M., Al-Marri, M., 2019a. Effect of rock mineralogy on hot-CO₂ injection for enhanced gas recover. *J. Nat. Gas Sci. Eng.* 72 (2019), 10303. <http://dx.doi.org/10.1016/j.jngse.2019.103030>.
- Martinez-Gomez, J., Nápoles-Rivera, F., Ponce-Ortega, J.M., El-Halwagi, M.M., 2017. Optimization of the production of syngas from shale gas with economic and safety considerations. *Appl. Therm. Eng.* 110, 678–685.
- Mastalerz, M., Drobnik, A., Rupp, J., 2014. Evaluation of geological characteristics of the new alban shale as a potential liquids from shale play in illinois basin. In: *Eastern Unconventional Oil and Gas Symposium*, Kentucky, U.S.A. Nov. 5–7. pp. 1–50.
- Maxwell, S., 2011. Microseismic hydraulic fracture imaging: the path toward optimizing shale gas production. *The Leading Edge* 30 (3), 340–346.
- McDonald, B., Wright, T.H., 2016. Completion optimization in fayetteville shale utilizing rate transient analysis for candidate selection. In: *SPE Hydraulic Fracturing Technology Conference*, Texas, U.S.A. Feb. 9–11. pp. 1–7.
- Murphy, E., Warner, M., Sarmah, B., 2013. A workflow to evaluate porosity, mineralogy and TOC in the utica-point pleasant shale play. In: *SPE Eastern Regional Meeting*, Pennsylvania, U.S.A. Aug. 20–22. pp. 1–20.
- Mustafa, A., Tariq, Z., Mahmoud, M., Radwan, A.E., Abdurhaheem, A., Abouelresh, M.O., 2022. Data-driven machine learning approach to predict mineralogy of organic-rich shales: An example from qusaiba shale, rub'al khali basin, Saudi Arabia. *Mar. Pet. Geol.* 137, 105495.
- Nadaraju, G., Elliott, D., 2010. Understanding Montney Reservoir Heterogeneity: A Geoengineering Approach, A Report. Encana Corporation, Calgary, Canada, p. 85.
- Naizhen, L.I.U., Guoyong, W.A.N.G., 2016. Shale gas sweet spot identification and precise geo-steering drilling in weiyuan block of sichuan basin, SW China. *Pet. Explor. Dev.* 43 (6), 1067–1075.
- Osamn, M.T., Bilgesu, I.H., 2015. Impact of geo-mechanical properties on the fracture treatment of utica shale. In: *Eastern Regional Meeting*, West Virginia, U.S.A. Oct. 13–15. Society of Petroleum Engineers, pp. 1–11.
- Parker, M., Buller, D., Petre, E., Dreher, D., 2009. Haynesville shale petrophysical evaluation. In: *Rocky Mountains Petroleum Technology Conference*, Colorado, USA, pp. 1–11.
- Passey, Q.R., Bohacs, K., Esch, W.L., Klimentidis, R., Sinha, S., 2010. From Oil-Prone Source Rock to Gas-Producing Shale Reservoir - Geologic and Petrophysical Characterization of Unconventional Shale Gas Reservoirs. Society of Petroleum Engineers, <http://dx.doi.org/10.2118/131350-MS>.
- Perry, F.V., Kelley, R.E., Dobson, P.F., Houseworth, J.E., 2014. Regional Geology: GIS Database for Alternative Host Rocks and Potential Siting Guidelines. Report # FCRD-UFD-2014-000068, pp. 168–170. (Retrieved July 10, 2016, from <https://energy.gov/ne/downloads/regional-geology-gis-database-alternative-host-rocks-and-potential-siting-guidelines>).
- Radwan, A.E., 2021. Modeling pore pressure and fracture pressure using integrated well logging, drilling based interpretations and reservoir data in the giant el morgan oil field, gulf of sues, Egypt. *J. Afr. Earth Sci.* 104165. <http://dx.doi.org/10.1016/j.jafrearsci.2021.104165>.
- Radwan, A.E., Abdelghany, W.K., Elkhawaga, M., 2021. Present-day in-situ stresses in Southern Gulf of Suez, Egypt: Insights for stress rotation in an extensional rift basin. *J. Struct. Geol.* 147 (104332), <http://dx.doi.org/10.1016/j.jsg.2021.104334>.
- Radwan, A.E., Abudeif, A.M., Attia, M.M., Elkhawaga, M.A., Abdelghany, W.K., Kasem, A.A., 2020. Geopressure evaluation using integrated basin modelling, well-logging and reservoir data analysis in the northern part of the badri oil field, gulf of sues, Egypt. *J. Afr. Earth Sci.* 162, 103743. <http://dx.doi.org/10.1016/j.jafrearsci.2019.103743>.
- Radwan, A.E., Abudeif, A.M., Attia, M.M., Mohammed, M.A., 2019. Pore and fracture pressure modeling using direct and indirect methods in badri field, gulf of sues, Egypt. *J. Afr. Earth Sci.* 156, 133–143. <http://dx.doi.org/10.1016/j.jafrearsci.2019.04.015>.
- Radwan, A.E., Wood, D.A., Mahmoud, M., Tariq, Z., 2022. Gas adsorption and reserve estimation for conventional and unconventional gas resources. In: *Sustainable Geoscience for Natural Gas Subsurface Systems*. Gulf Professional Publishing, pp. 345–382.
- Reeves, R.S., Hill, D.G., Cox, O.D., 1993. Production optimization in the antrim shale. In: *Production Operations Symposium*, Oklahoma, USA, pp. 1–11.
- Rickman, R., 2008. A practical use of shale petrophysics for stimulation design optimization: All shale plays are not clones of the barnett shale. In: *SPE Annual Technical Conference and Exhibition*, Denver, Colorado, USA, SPE 115258-MS.
- Rivera, S., Saidian, M., Godinez, J.L., Prasad, M., 2014. Effect of mineralogy on NMR, sonic, and resistivity: A case study of Monterey formation. In: *Unconventional Resources Technology Conference (URTEC)* Colorado, USA, pp. 1–20.
- Roberts, D.F., 2013. Identifying and Mapping Clay-Rich Intervals in the Fayetteville Shale: Influence of Clay on Natural Gas Production Intervals (M.Sc. Thesis). The University of Texas, Austin, p. 53.
- Robison, C., Smith, M., Royle, R., 1999. Organic facies in cretaceous and jurassic hydrocarbon source rocks, southern indus basin, Pakistan. *Int. J. Coal Geol.* 39 (1–3), 205–225. [http://dx.doi.org/10.1016/s0166-5162\(98\)00046-9](http://dx.doi.org/10.1016/s0166-5162(98)00046-9).
- Rokosh, D.C., Beaton, A., Pawlowicz, J., Anderson, S., Berhane, M., 2010. Mineralogy of Duvernay, Muskwa, and Montney Formations for Shale Gas Resource Evaluation. Report Summary. Geo-Canada/Alberta Geological Survey, p. 2.
- Ruotsala, A., 1980. Mineralogy of Antrim Shale, Michigan. Report # FE-2346-79, Dow Chemical Co., Midland, MI, USA, p. 2, (Retrieved April 10, 2016, from <http://www.osti.gov/scitech/biblio/5201912>).

- Saddique, B., Ali, N., Irfan, U., Hanif, M., Shah, A.S., Saleem, I., Faizi, M.M., Yasir, M.A., 2016. Petrophysical analysis of the reservoir intervals in kahi-01 well, kohat sub-basin, Pakistan. *J. Himal. Earth Sci.* 49 (1), 30–40.
- Salehi, A.I., 2009. New Albany Shale Gas Project, a Joint Research Project. Annual Progress Report, Gas Technology Institute USA, p. 40.
- Sarg, F.J., 2012. The Bakken – an Unconventional Petroleum and Reservoir System. Final Scientific/Technical Report, Colorado School of Mines, USA, p. 65.
- Shah, M.S., Ahmad, N., Ahmad, N., Ahsan, N., 2013. The mineralogical and petrographical studies of the lithofacies of the hangu formation in the salt range, Punjab, Pakistan. *Pak. J. Sci.* 65 (1), 142–149.
- Shahzad, A., 2007. Identification of Potential Hydrocarbon Source Rocks using Biological Markers in Kohat Plateau, North Pakistan (M.Sc. Thesis). National Center of Excellence in Geology, University of Peshawar, Pakistan.
- Sheikh, N., Gao, P.H., 2017. Evaluation of shale gas potential in the lower cretaceous sembar formation, the southern indus basin, Pakistan. *J. Nat. Gas Sci. Eng.* 44, 162–176. <http://dx.doi.org/10.1016/j.jngse.2017.04.014>.
- Shu, Y., Lu, Y., Chen, L., Wang, C., Zhang, B., 2020. Factors influencing shale gas accumulation in the lower silurian longmaxi formation between the north and south jiaoshiba area, southeast sichuan basin, China. *Mar. Pet. Geol.* 111, 905–917.
- Siddiqui, I.F., Adhami, A., Asghar, A., Hussain, A., Khan, W.M., 2014. Shale gas potential of the lower goru formation over the lakhra high in lower indus basin, Pakistan. In: AAPG Annual Convention and Exhibition, Pittsburgh, Pennsylvania, USA. pp. 1–28.
- Soeder, J.D., 2011. Petrophysical characterization of the marcellus & other gas shales. In: AAPG Eastern Section Meeting, Arlington, Virginia, USA, Sep. 28. pp. 1–35.
- Sohail, G.M.D., 2020. Literature Review: An Overview of Pakistani Shales for Shale Gas Exploration and Comparison to North American Shale Plays. An Evaluation of Geomechanical Properties of Potential Shale Gas Reservoirs in the Lower Indus Basin, Pakistan. USASK, Canada.
- Soltanzadeh, M., Fox, A., Rahim, A., 2015. Application of an Integrated Approach for the Characterization of Mechanical Rock Properties in the Duvernay Formation. *Geo-Convention*, Calgary, Canada, pp. 1–4.
- Sondergeld, C., Newsham, K., Comisky, J., Rice, M., Rai, C., 2010. Petrophysical considerations in evaluating and producing shale gas resources. In: Proceedings of SPE Unconventional Gas Conference. <http://dx.doi.org/10.2523/131768-ms>.
- Sone, H., Zoback, M.D., 2013a. Mechanical properties of shale gas reservoir rocks – Part 1: Static and dynamic elastic properties and anisotropy. *Geophysics* 78 (this issue), <http://dx.doi.org/10.1190/geo2013-0050.1>.
- Sone, H., Zoback, D.M., 2013b. Mechanical properties of shale-gas reservoir rocks – Part 1: Static and dynamic elastic properties and anisotropy. *Geophysics* 78 (5), 381–392.
- Song, Y., Li, Z., Jiang, L., et al., 2015. The concept and the accumulation characteristics of unconventional hydrocarbon resources. *Pet. Sci.* 12 (4), 563–572. <http://dx.doi.org/10.1007/s12182-015-0060-7>.
- Taylor, K.G., Macquaker, J.H.S., 2014. Diagenetic alterations in a silt- and clay rich mudstone succession: an example from the upper cretaceous mancos shale of Utah, USA. *Clay Miner.* 49, 213–227. <http://dx.doi.org/10.1180/claymin.2014.049.2.05>.
- Tian, H., Xiao, X.M., Yang, L.G., Xiao, Z.Y., Guo, L.G., Shen, J.G., 2009. Pyrolysis of oil at high temperatures: Gas potentials, chemical and carbon isotopic signatures. *Chin. Sci. Bull.* 54, 1217–1224.
- Ucok, H., 1988. A sensitivity study on the geological factors influencing the oil recovery from the Monterey formation. In: 63rd Annual Technical Conference and Exhibition of the Society of Petroleum Engineers, Houston, Texas, USA. pp. 1–8.
- US EIA, 2011. Review of Emerging Resources: U.S. Shale Gas and Shale Oil Plays, a Report. Energy Information Administration, p. 105.
- US EIA, 2015. Technically Recoverable Shale Oil and Shale Gas Resources: Canada, India and Pakistan, a Report. Energy Information Administration (EIA), p. 42, (Retrieved 2016, from https://www.eia.gov/analysis/studies/worldshalegas/pdf/India_Pakistan_2013-15.pdf).
- Vengosh, A., Warner, N., Jackson, R., Darrah, T., 2013. The effects of shale gas exploration and hydraulic fracturing on the quality of water resources in the United States. *Procedia Earth Planet. Sci.* 7, 863–866.
- Walls, D.J., Morcote, A., 2015. Quantifying variability of reservoir properties from a wolfcamp formation core. In: Unconventional Resource Technology Conference, San Antonio, Texas, USA. pp. 1–10.
- Walls, D.J., Morcote, A., Dvorkin, J., 2016. Describe the elastic rock properties revealed by whole core-CT scanning of samples from the wolfcamp formation. In: *Understanding Rock Properties*. Oilfield Technology, USA, pp. 60–64.
- Walls, J.D., Sinclair, S.W., 2011. Eagle Ford shale reservoir properties from digital rock physics. *First Break* 29 (6), <http://dx.doi.org/10.3997/1365-2397.29.6.51280>.
- Walter, S., Beavis, K., Whibbs, C., Stricker, S., Preston, A., Jenkins, J., Hein, F., 2016. Recognizing duvernay B-carbonate distribution and its potential implications on resource and reserve estimations. In: AAPG Conference & Exhibition, Calgary, Canada. pp. 1–2.
- Wandrey, C.J., Law, B.E., Shah, H.A., 2004. Sembar Goru/Ghazij Composite Total Petroleum System, Indus and Sulaiman-Kirthar Geologic Provinces, Pakistan and India. *U.S. Geological Survey Bulletin*, 2208-C, USA, p. 29.
- Wang, F.P., Gale, J.F.W., 2009. Screening criteria for shale-gas systems. *Gulf Coast Assoc. Geol. Soc. Trans.* 59, 779–793.
- Wang, Q., Wang, L., 2016. Comparative study and analysis of the development of shale gas between China and the USA. *Int. J. Geosci.* 7, 200–209.
- Warwick, D.P., Javed, S., Tahir, A.S., Shakoor, T., Khan, M.A., Khan, L.A., 1995. Lithofacies and palynostratigraphy of some cretaceous and paleocene rocks, surghar and salt range coal fields, northern Pakistan. *US Geol. Bull.* 2096, 29.
- Wenzhi, Z., Ailin, J., Yunsheng, W., Junlei, W., Hanqing, Z., 2020. Progress in shale gas exploration in China and prospects for future development. *China Pet. Explor.* 25 (1), 31.
- Xie, R., Zhou, W., Liu, C., Yin, S., Radwan, A.E., Lei, W., Cai, W., 2022. Experimental investigation on dynamic and static rock mechanical behavior, failure modes and sequences of frequent interbedded sand and shale reservoirs. *Interpretation* 10 (3), 1–52.
- Xin, C., Chen, L., Guo, X., Wang, C., 2019. Geochemical characteristics of shale gas in the silurian longmaxi formation, jiaoshiba area, southeast sichuan basin, China. *Energy Fuels* 33 (9), 8045–8054.
- Zhang, H., Shi, J., Li, X., 2018. Optimization of shale gas reservoir evaluation and assessment of shale gas resources in the oriente basin in Ecuador. *Pet. Sci.* 15 (4), 756–771. <http://dx.doi.org/10.1007/s12182-018-0273-7>.
- Zou, C., Dong, D., Wang, S., Li, J., Li, X., Wang, Y., Li, X., Wang, Y., Li, D., Cheng, K., 2010. Geological characteristics and resource potential of shale gas in China. *Pet. Explor. Dev.* 37 (6), 641–653.
- Zuber, et al., 2002. A Comprehensive Reservoir Evaluation of a Shale Reservoir-The New Albany Shale. SPE Annual Technical Conference and Exhibition, San Antonio, Texas SPE 77469-MS.